A Modular Approach to Polymer Architecture Control via Catenation of Prefabricated Biomolecular Segments: Polymers Containing Parallel β-Sheets Templated by a Phenoxathiin-Based Reverse Turn Mimic

Michael J. Winningham and Dotsevi Y. Sogah*

Department of Chemistry, Baker Laboratory, Cornell University, Ithaca, New York 14853-1301

Received June 4, 1996; Revised Manuscript Received December 16, 1996[⊗]

ABSTRACT: A biomolecular Lego set modular method whereby prefabricated building blocks are linked block by block has been developed and applied to the synthesis of peptide-based polymers containing parallel β-sheets induced by phenoxathiin derivatives acting as reverse turn mimics. Spectroscopic studies show that phenoxathiin is an effective template for β-sheet formation allowing even weak hydrogen acceptors such as ester amides to exist almost exclusively in intramolecularly hydrogen-bonded conformations. Replacing the phenoxathiin derivative with flexible hydrocarbon chains results in substantial loss of intramolecular hydrogen bonding. Solid state FTIR of the polymers revealed that the expected parallel β-sheets were retained in the polymer solely due to the presence of the rigid phenoxathiin template. Conformationally unrestricted units incapable of inducing sheet formation provide mostly random coils and contribute to interchain and intersheet antiparallel hydrogen bonding. The nature of the β-sheet domains has been confirmed through study of model octapeptides. DSC and TGA studies reveal that as the flexibility of the linkers decreases T_g and onset decomposition temperature also decrease. Powder X-ray diffraction of the unoriented polymers shows that they are semicrystalline.

Introduction

Biopolymers such as proteins are characterized by the occurrence of conformationally defined secondary and tertiary structures.[1] These higher order structures are a result of secondary interactions between various amino acid residues along the protein primary chain. However, such highly ordered structures are rare in synthetic polymers. The ultimate goal of the synthetic polymer chemist is to precisely control polymer architecture in order to obtain materials with well-defined properties. Nature does this routinely in the biosynthesis of proteins, where sequence and molecular weight and, in fact, overall architecture, are strictly controlled. In contrast, the current methods for polymer synthesis do not have the capabilities for precise structure control despite the enormous advances that are being made in living polymerization methods.[2] For example, it is not currently possible to precisely control monomer sequence, and the polymer chains cannot be induced to fold predictably. Hence, in the search for the appropriate synthetic approach to multidimensional assemblies, one may have to turn to lessons learned from nature.

One technique for obtaining polymers of controlled sequence and predictable chain-folding characteristics involves the use of DNA templates.[3,4] We report herein a modular chemical approach in which prefabricated, sequence-specific, conformationally ordered building blocks are assembled block by block into a polymeric supermolecular structure. This chemical Lego set approach offers the opportunity for controlling the microstructure of synthetic polymers and incorporation of appropriately decorated building blocks that can be tailored to specific functions and properties. Hard segments consisting of peptide strands with a high propensity to form well-ordered β-sheets are incorporated. Capability for predictable chain folding is provided through incorporation of rigid organic, nonpeptide reverse turn mimics. This technique has the potential of providing new materials with unique mechanical and physical properties through the incorporation of hard and soft segments selected from the large repertoire of synthetic polymers.

There has been a resurgence of activity in the preparation and study of synthetic antiparallel β-sheets in recent years.[5−7] Rigid turn mimics are used to restrict the conformational freedom of attached peptides and serve as nucleation centers for inducing secondary structure through hydrogen bonding.[7] Despite the increased activity in the study of β-sheet structures, there has been very little effort to date in the preparation and study of parallel β-sheets.[8,9] In natural systems, the formation of parallel β-sheet structures requires bringing together remote peptide segments into a location where formation and interactions of parallel β-strands can take place. Hence, parallel β-strands in a sheet conformation can only be linked by large peptide loops or helices, unlike antiparallel β-strands which may be linked by β-turns.[10] We have recently shown that phenoxathiin could serve as templates for parallel β-sheets.[8] This technique of substituting a rigid peptidomimetic for the flexible peptide loop has now been applied to synthesis of parallel β-sheets which are subsequently incorporated into synthetic polymers. The goal is to obtain hybrid polymers that combine synergistically the properties of natural and synthetic polymers.

There are many fibrous proteins that have repetitive peptide sequences which fold into regular structural elements that define the properties of the biopolymer and can serve as excellent model systems for synthetic polymers of controlled structures.[1,11,12] These include keratin,[1] collagen,[1] fibronectin,[1] silks,[12] elastin,[13] and amelogenins.[14] Silk fibroin, for example, consists of hard, crystalline regions of antiparallel β-sheets and irregular, amorphous regions, while nylon-6,6 and poly(*p*-phenyleneterephthalamide) (PPTA; U.S. trade name

[⊗] Abstract published in *Advance ACS Abstracts,* February 1, 1997.

S0024-9297(96)00804-2 CCC: $14.00

Chart 1

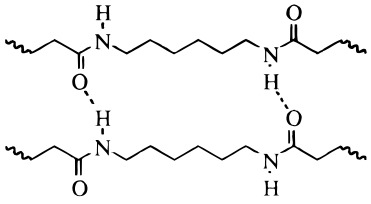

Nylon-6,6

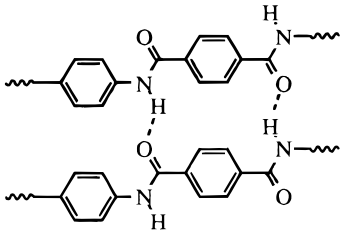

Poly(*p*-phenylene terephthalamide)

Scheme 1

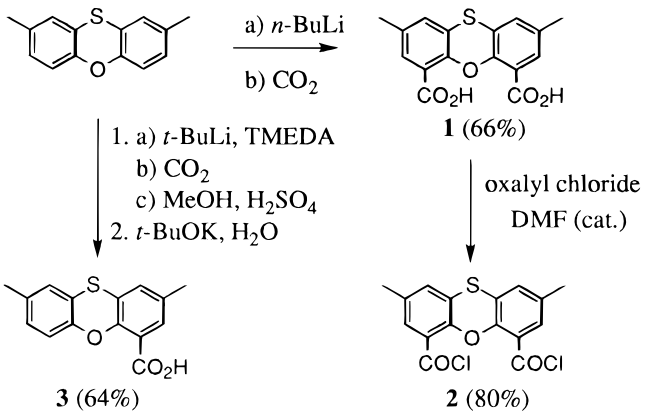

Kevlar) exist as stacks of parallel hydrogen-bonded sheets as shown in Chart 1.[15] In our attempts at preparing silk-based polymers by catenation of preformed building blocks, we chose the GlyAlaGlyAla (GAGA) sequence which is structurally similar to the repeating sequence found in the β-sheet domains of *Bombyx mori* silk fibroin, i.e., [GAGAGSGAAG(SGAGAG)$_8$].[12] This permits the properties of the new polymers to be compared qualitatively with those of the silk materials. The folded structures are templated by phenoxathiin derivatives, and the first amino acid attached to the rigid nucleus is Gly which provides flexibility since it permits a broader range of allowable NH−CαH dihedral angles.[16]

Results and Discussion

Synthesis of the Building Blocks. 2,8-Dimethylphenoxathiin-4,6-dicarboxylic acid (**1**) was synthesized from 2,8-dimethylphenoxathiin[17] via treatment with *n*-butyllithium in THF followed by cannulation of the dianion solution onto solid CO_2 to give the diacid **1** in 66% yield (Scheme 1). Reaction of the diacid with oxalyl chloride in the presence of a catalytic amount of DMF gave the dicarbonyl chloride **2** in 80% yield after recrystallization from hexanes. 2,8-Dimethylphenoxathiin-4-carboxylic acid (**3**) was synthesized from **1** in two steps in 64% overall yield.[18] The synthesis of 2,8-dimethyl-4,6-bis(aminomethyl)phenoxathiin-10,10-dioxide (**4**) from 2,8-dimethylphenoxathiin was accomplished in three steps through modification of literature procedures.[9b] The required tetrapeptide BOC-GAGA-OH was prepared in quantitative yield by catalytic hydrogenolysis over Pd/C of the corresponding benzyl ester which was prepared by standard peptide synthesis in solution. Attachment of BOC-GAGA-OH to the various diamines via DCC/HOBT coupling gave the novel BOC-protected octapeptide monomers **5** (64%), **7a** (81%), **7b** (72%), **7c** (72%), and **7d** (99%) (Schemes 2 and 3). Purification was accomplished by continuous Soxhlet extraction with acetone.

Scheme 2

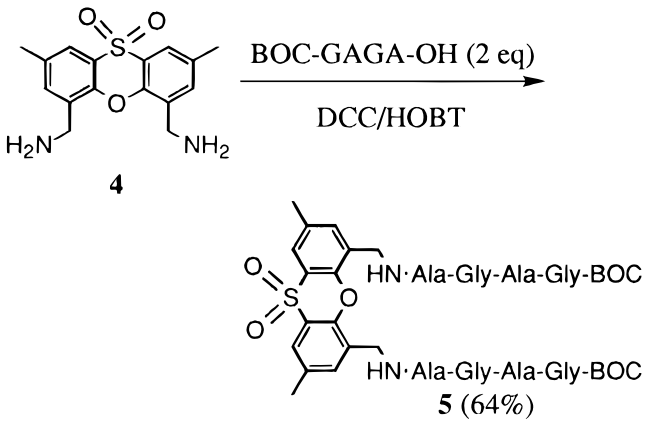

Scheme 3

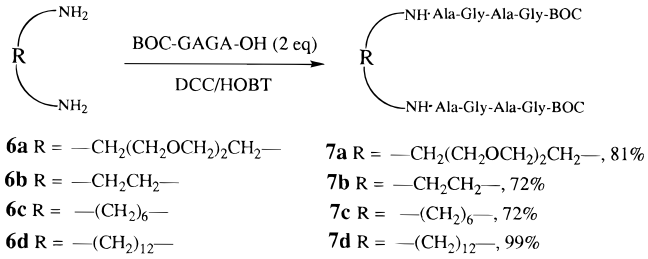

6a R = —$CH_2(CH_2OCH_2)_2CH_2$—
6b R = —CH_2CH_2—
6c R = —$(CH_2)_6$—
6d R = —$(CH_2)_{12}$—

7a R = —$CH_2(CH_2OCH_2)_2CH_2$—, 81%
7b R = —CH_2CH_2—, 72%
7c R = —$(CH_2)_6$—, 72%
7d R = —$(CH_2)_{12}$—, 99%

Scheme 4

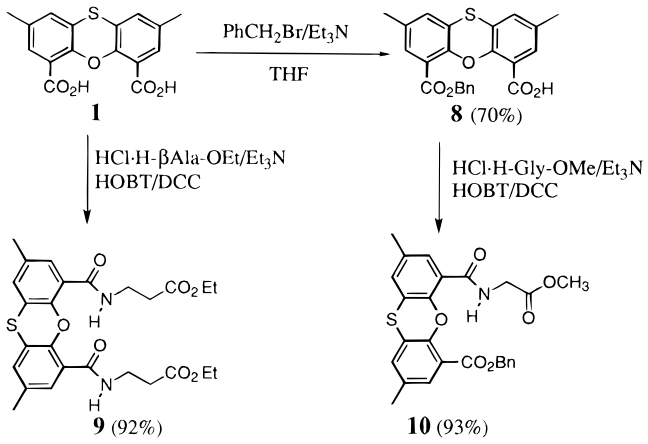

Standard DCC/HOBT coupling of β-Ala-OEt to **1** gave **9** in 92% yield (Scheme 4). Treatment of **1** with benzyl bromide in the presence of triethylamine gave the monobenzyl ester **8** (70%) which was subsequently converted to **10** (93%) by reaction with Gly-OMe in the presence of DCC/HOBT. Similarly, the coupling of Gly-OMe to **1** gave **11** in 73% yield (Scheme 5), while the degenerate two-arm peptide **13** was obtained from **1** in 65% in yield. Reaction of **3** with the appropriately protected peptide gave the one-arm models **12** and **14** in 75% and 54% yields, respectively (Scheme 6).

Scheme 5

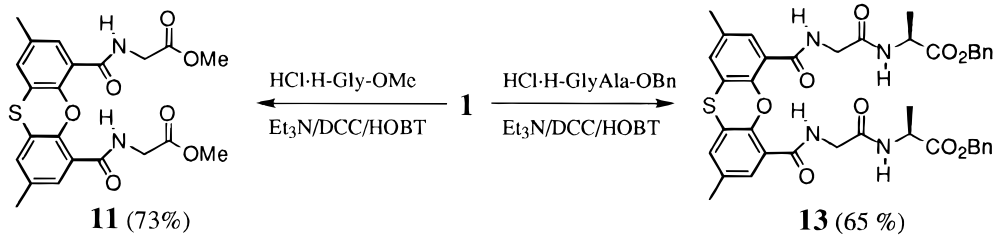

Scheme 6

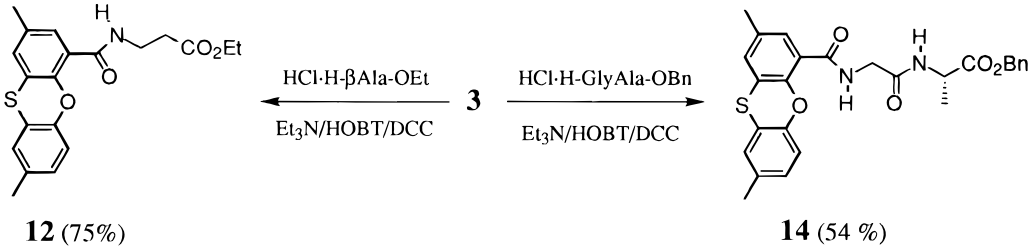

Spectroscopic Evidence for Nucleation of Parallel Sheets. FTIR spectroscopy of the NH stretching region (3200−3500 cm^{-1}) is a useful technique for obtaining information about hydrogen bonding and aggregation in peptide derivatives in dilute CH_2Cl_2 solutions.[19] We have previously established the ability of **9** to nucleate a parallel 10-membered ring hydrogen bond in CH_2Cl_2.[8] The FTIR spectrum of **9** showed a peak at 3429 cm^{-1} corresponding to a free NH and a peak at 3373 cm^{-1} corresponding to a hydrogen-bonded NH. The relative intensities of both peaks were found to be constant throughout the concentration range studied suggesting that **9** did not aggregate under the conditions of the experiment and that the observed hydrogen bonding was intramolecular. In contrast, the FTIR spectrum of **12** showed only a single concentration independent peak at 3434 cm^{-1}. In our current investigations, we found that compound **11**, in which Gly has been substituted for β-alanine, also existed in an intramolecular hydrogen-bonded state as shown in Figure 1a. Furthermore, the FTIR spectrum of ester amide **10** shows only one broad peak centered at 3378 cm^{-1} indicating that **10** exists exclusively in an intramolecular hydrogen-bonded conformation (Figure 1b) despite esters being weaker hydrogen acceptors than amides.[19] These results support the facile formation of the 10-membered ring and confirm the effectiveness of a phenoxathiin nucleus as a hairpin turn mimic.

Dependence of chemical shifts of amide NH's on temperature has been used to distinguish between hydrogen-bonded and free NH's in peptides and related amides.[7a,b,e,8,19−21] In apolar organic solvents, a small value of the temperature dependence coefficient, $-\Delta\delta/\Delta T$, indicates either a free NH or one that remains hydrogen bonded throughout the temperature range, while a large value always reflects an initially shielded NH that becomes exposed. However, the results of variable temperature NMR studies (Table 1) show that both compounds **9** and **12** gave low $-\Delta\delta/\Delta T$ values (2.7 and 3.3 ppb/K, respectively) even though **9** was shown to be intramolecularly hydrogen bonded and **12** was not hydrogen bonded at all in CD_2Cl_2.[8] This lack of one-to-one correspondence renders an unambiguous use of $-\Delta\delta/\Delta T$ obtained in apolar solvents very difficult.[20] Hence, we were unable to distinguish between the hydrogen-bonded and free β-alanine NH's on the basis of only $-\Delta\delta/\Delta T$ values obtained in CD_2Cl_2.

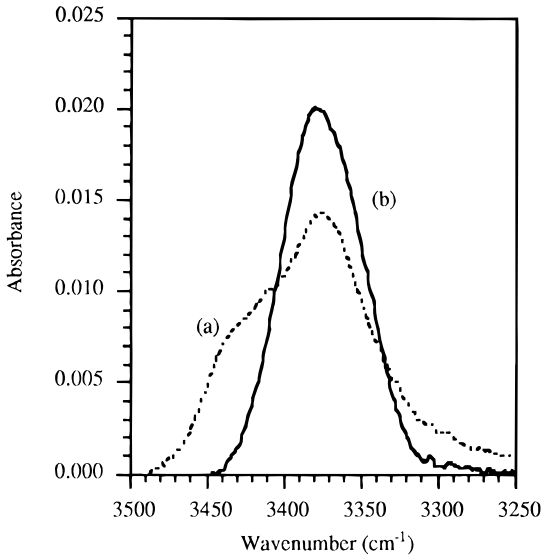

Figure 1. FTIR spectra for the NH stretching region of **10** and **11** in CH_2Cl_2 at room temperature after subtraction of the spectrum of pure CH_2Cl_2: (a) 1.5 mM **11**, cell path length = 0.5 mm; (b) 2.0 mM **10**, cell path length = 0.5 mm. Spectra were recorded on a Perkin Elmer 16PC spectrometer.

Table 1. Variable Temperature ^{1}H NMR Studies in CD_2Cl_2 and DMSO-d_6

		$-\Delta\delta/\Delta T$ (ppb/K)	
compd no.	amide NH	CD_2Cl_2[a]	DMSO-d_6[b]
9	βAla-NH's	2.7[c]	3.2
12	βAla-NH	3.3[c]	4.2
13	Gly-NH's	1.6	3.7
13	Ala-NH's	5.1	5.8

[a] The temperature was varied from 193 to 293 K. Peptide concentrations in CD_2Cl_2 were ≤2.0 mM. [b] The temperature was varied from 303 to 373 K. Peptide concentrations in DMSO-d_6 were ≤5.5 mM. [c] Taken from ref 8.

In polar aprotic solvents such as DMSO-d_6, $-\Delta\delta/\Delta T$ values > 5 ppb/K are typical for a solvent-exposed NH while values < 3 ppb/K suggest an amide NH that is shielded from solvent through either intramolecular hydrogen bonding or steric shielding.[22] The amide NH of **9** gave $-\Delta\delta/\Delta T$ = 3.2 ppb/K which is consistent with degenerate hydrogen-bonded structures that are rapidly interconverting on the NMR time scale (Table 1). Compound **12** gave an intermediate $-\Delta\delta/\Delta T$ = 4.2

Scheme 7

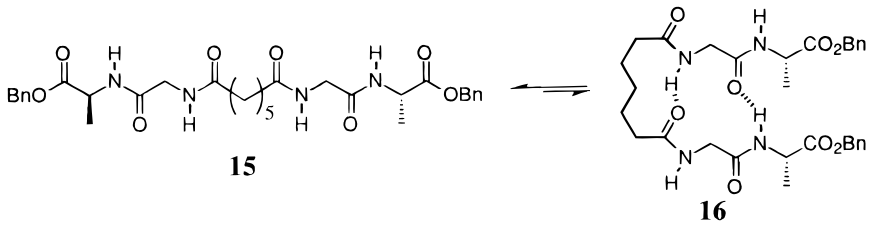

15 **16**

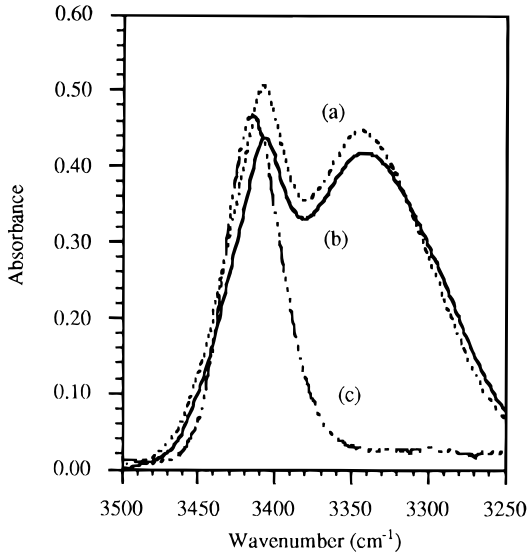

Figure 2. FTIR spectra for the NH stretching region of **13** and **14** in CH_2Cl_2 at room temperature after subtraction of the spectrum of pure CH_2Cl_2: (a) 0.97 mM **13**, expanded 20×; (b) 19.5 mM **13**; (c) 1.1 mM **14**, expanded 20×. Baseline has been corrected for spectrum c. Spectra were recorded on a Perkin Elmer 16PC spectrometer; cell path length = 1 mm.

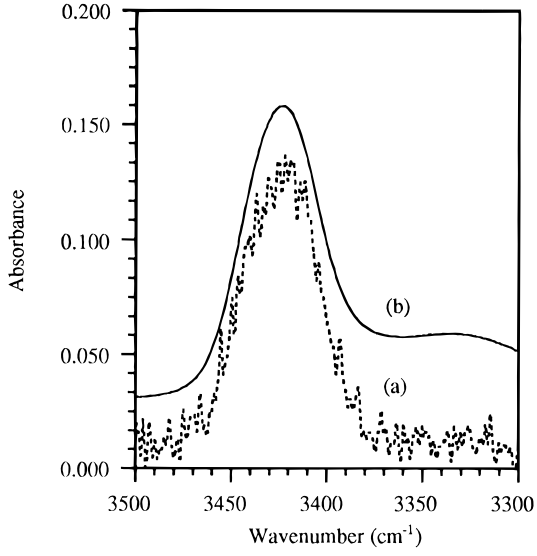

Figure 3. FTIR spectra for the NH stretching region of **16** in CH_2Cl_2 at room temperature after subtraction of the spectrum of pure CH_2Cl_2: (a) 0.081 mM **16** expanded 70x; (b) 3.9 mM **16**. Baseline has been corrected for spectra (a) and (b). Spectra were recorded on a Perkin Elmer 16PC spectrometer; cell pathlength = 1 mm.

ppb/K which is lower than expected for a non-hydrogen-bonded NH. This may be due to steric shielding by the phenoxathiin ring system.

Spectroscopic Evidence for Propagation of Hydrogen Bonding in a Parallel Fashion. The FTIR spectrum of **13** (Figure 2a,b) shows two sets of concentration independent NH peaks at 3407 cm^{-1} (free NH) and 3342 cm^{-1} (hydrogen-bonded NH). In contrast, the FTIR spectrum of the one-arm model **14** (Figure 2c) shows only one peak in the NH stretching region at 3415 cm^{-1}, indicating the absence of any kind of hydrogen bonding. The need for a rigid template was demonstrated by the observation that the flexible linear peptide **15** (Scheme 7), which could form a 10-membered ring-nucleated sheet structure (**16**), existed predominantly in the non-hydrogen-bonded state. Thus, its FTIR spectrum (Figure 3) shows largely a free NH stretching peak at 3424 cm^{-1} and only a very small and broad hydrogen-bonded peak at 3336 cm^{-1}.

^1H NMR investigation of **9** and **13** revealed that both compounds exist in fast interconverting degenerate conformations. Thus, only one peak per each type of NH (both β-Ala-NH's at δ 7.62 for **9**, both Gly-NH's at δ 7.86 in **13**, and both Ala-NH's at δ 7.27 in **13**) was observed. In CD_2Cl_2, the Ala-NH's of **13** (Table 1) gave a much greater response to temperature ($-\Delta\delta/\Delta T = 5.1$ ppb/K) than the NH's closest to the aromatic nucleus ($-\Delta\delta/\Delta T = 1.6$ ppb/K) even though both are intramolecularly hydrogen bonded (FTIR evidence). The observed smaller than expected responses are attributed to steric shielding and to the structures existing in fast equilibrating degenerate conformations where for every hydrogen-bonded NH there is an equivalent and identical free NH with which it can exchange. In DMSO-d_6 (Table 1) the $-\Delta\delta/\Delta T$ value for the Gly-NH's of **13** was 3.7 ppb/K, consistent with a hydrogen-bonded structure involving the adjacent Gly residues. The $-\Delta\delta/\Delta T$ value of 5.8 ppb/K obtained for the degenerate Ala-NH's suggests that in DMSO-d_6 their hydrogen bonds are more readily disrupted by the polar solvent, which is consistent with Ala being the terminal residue and therefore more solvent accessible. Since the FTIR spectroscopic results suggest the existence of intramolecular hydrogen bonds, the small $-\Delta\delta/\Delta T$ values are an indication that the enthalpies of the various equilibrating conformations under the conditions of our experiments are rather similar.

Unlike variable temperature experiments in apolar solvents, DMSO titration studies tend to provide less ambiguous information regarding the hydrogen-bonding character of an amide NH.[22b,e] Figure 4 shows the chemical shift changes upon addition of DMSO-d_6 for **13**. The observed response of Ala-NH's is consistent with the results of both the variable temperature and FTIR studies which suggest that these NH's are hydrogen bonded.

Catenation of Preformed β-Sheets into Peptide Hybrid Polymers. Having established the facile formation of sheet structures templated by the rigid phenoxathiin group, we directed our attention to their incorporation into silklike and nylonlike polymers. The polymers could be made by either the interfacial or solution condensation method. There are two possible routes (A and B in Scheme 8) to these polymers. Our

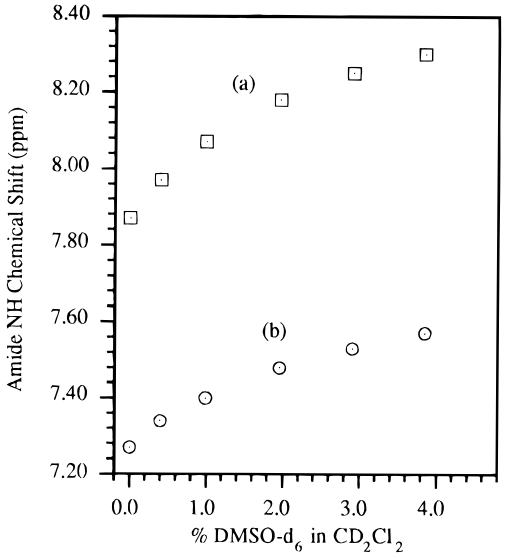

Figure 4. Solvent composition dependencies of amide proton chemical shifts of **13** (0.33 mM) in CD_2Cl_2 as DMSO-d_6 is added at 23.5 °C: (a) Gly-NH's; (b) Ala-NH's. Chemical shifts were referenced to residual $CHDCl_2$ (5.32 ppm). Chemical shifts for amide NH of **13** (1 mM) in 100% DMSO-d_6 at 30.0 °C: 8.78 ppm (Gly-NH's), 8.34 ppm (Ala-NH's). Spectra were obtained on a Varian Unity 500 MHz spectrometer.

Scheme 8

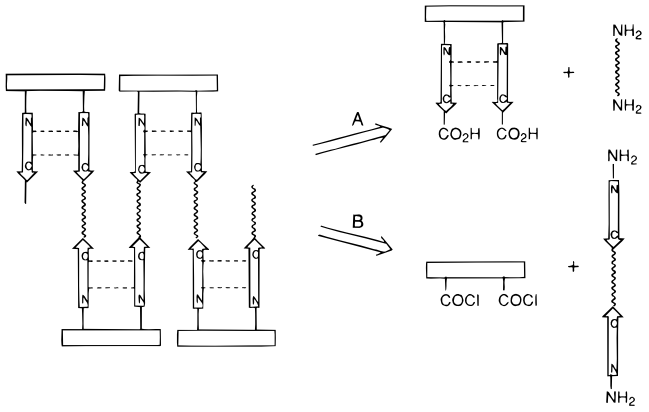

initial choice was route A which involves using the preformed parallel sheet monomers and a suitable diamine in accordance with our Lego concept. However, we found that our prefabricated parallel β-sheets templated by the phenoxathiindicarbonyl moiety are very insoluble in most solvents. Hence, we resorted to route B which entails attaching the peptides to either flexible linkers or units with no or low propensity for inducing sheet formation for increased solubility. The polymers that would form upon polymerization of the acid chloride derivative of the rigid β-turn mimic would have the same structure and sequence as those from route A. Five of such peptides (**5**, **7a**−**d**, Schemes 2 and 3) were prepared as described earlier. Using building blocks with potentially higher solubility provides the opportunity to compare the results of interfacial techniques with those of solution polymerization.

Interfacial Polymerization. One major advantage that interfacial polymerization provides is that it gives high molecular weight polymers from AA and BB monomers at ambient temperature since the critical stoichiometric balance between the two monomers is readily achieved at the interface of the two immiscible solvents. The diamine (BB monomer) is dissolved in water containing an inorganic base, while the diacid

Scheme 9

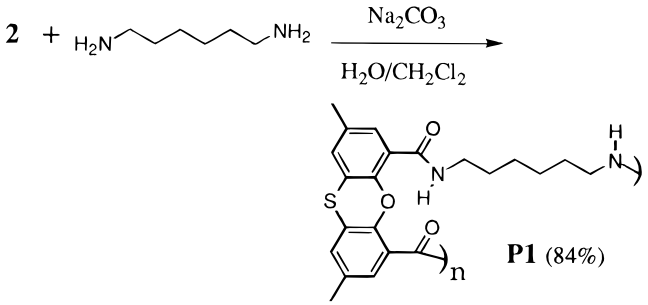

Table 2. Polyamides P1−P5 Prepared via Interfacial Polymerization[a]

polymer	[mon] (M)	time (h)	yield (%)	η_{inh}[b] (dL/g)
P1	0.210	7	84	0.16
P2	0.027	72	57	0.11[c]
P4	0.092	48	46	0.14
P5	0.130	48	82	0.21
P3	0.200	96	50	0.19

[a] Polymerizations were carried out in CH_2Cl_2/H_2O mixture at room temperature. [b] Inherent viscosities measured in dichloroacetic acid at 25.0 °C and a concentration of 0.5 g/dL. [c] Inherent viscosity measured at 0.4 g/dL.

chloride (AA monomer) is dissolved in a water-immiscible organic solvent. The formation of the polymer occurs at the interface between the two solvents by the extremely fast Schotten−Baumann reaction. This technique contrasts with standard solution step-growth polymerization where the critical stoichiometric balance between the AA and BB monomers can be difficult to achieve.

To determine the appropriate interfacial polymerization reaction conditions for our systems, 2,8-dimethylphenoxathiin-4,6-dicarbonyl chloride (**2**) and hexamethylenediamine were reacted using CH_2Cl_2 as one phase and aqueous Na_2CO_3 as the other. The polymer precipitated immediately at the CH_2Cl_2/H_2O interface and was collected and washed with H_2O and MeOH to give the novel nylonlike polyamide **P1** in 84% yield (Scheme 9). **P1** was insoluble (<1 mg/mL) in methanol, TFE, DMF, DMSO, NMP, and formic acid but dissolved readily in HFIP, TFA, dichloroacetic acid, and sulfuric acid. Inherent viscosity measured in dichloroacetic acid was found to be 0.16 dL/g (Table 2). Optimization of reaction conditions has not yet been performed in these preliminary studies since the initial objective is to demonstrate the feasibility of the concept. It is known that slight changes in reaction conditions such as solvent composition, temperature, and monomer concentration can have profound effects on the molecular weight and other properties of the polymers.[23] Polymers with kinks incorporated into their structures tend to form less viscous solutions than flexible linear polymers due to their reduced hydrodynamic volumes.[23e,f] Hence, the low viscosities reported herein do not necessarily indicate low molecular weights.

The method was applied to the synthesis of the silklike folded polyamide **P2**. Monomer **5** was deprotected by treatment with TFA for 2 h and concentrated to an oily residue (Scheme 10). Addition of HCl (3.8 M in 1,4-dioxane) precipitated the diamine·HCl **17** in quantitative yield.[23] The diamine salt was neutralized with Et_3N in DMF, and the free diamine monomer was redissolved in DMF and diluted with H_2O. The monomer and dicarbonyl chloride **2** were subjected to interfacial polymerization using $CH_2Cl_2/H_2O/Na_2CO_3$ (Scheme

Scheme 10

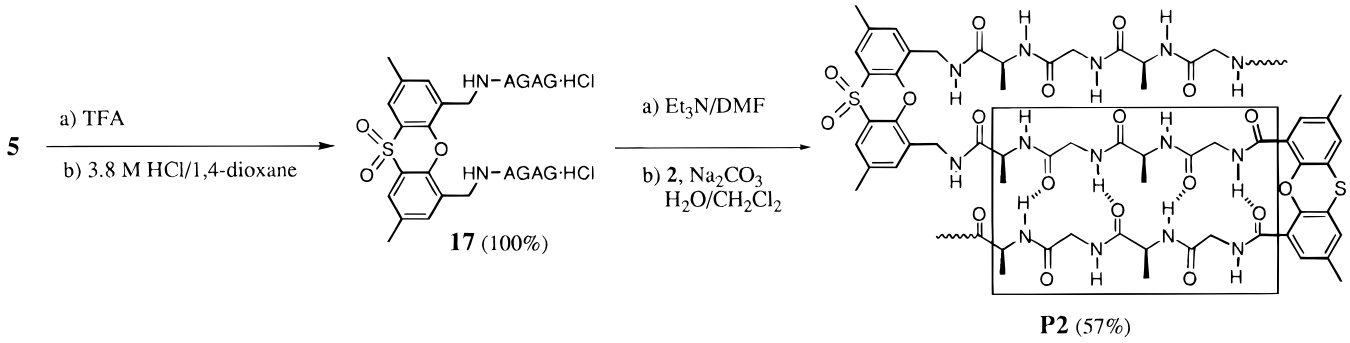

Scheme 11

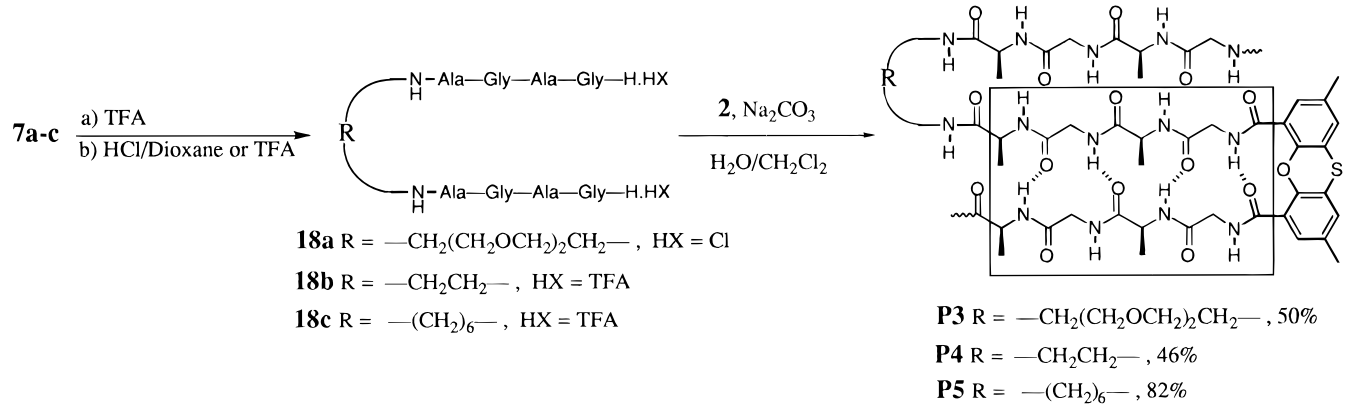

10). The formation of the polymer **P2** (57%) was instantaneous as evidenced by the immediate precipitate formation at the CH_2Cl_2/H_2O interface. Similarly, **P3**, **P4**, and **P5** were prepared using **7a**−**c**, respectively (Scheme 11). Diamine monomer **18d** was found to be insoluble in water, so **P6** was not synthesized interfacially. For **P4** and **P5** the TFA salts **18b**,**c** were used directly. The boxed region of the polymer represents the expected parallel β-sheet conformation for each system. The peptide strands attached to either the flexible linkers for **P3**−**P5** or the nonplanar linker 2,8-dimethyl-4,6-bis(aminomethyl)phenoxathiin 10,10-dioxide for **P2** are not expected to form intrastrand hydrogen-bonded parallel sheets.[7c,d] We have already shown that tetrapeptide **15** containing a flexible linker showed little or no tendency to form β-sheets.

The polymers exhibited limited solubility in common organic solvents as expected due to strong inter- and intrachain interactions. For example, the hybrid polymer **P2** was insoluble in methanol, TFE, and DMF, slightly soluble in DMSO, NMP, and HFIP but completely soluble in formic acid, TFA, and sulfuric acid. **P3** was insoluble in methanol and TFE, slightly soluble in DMSO, NMP, and DMF, and very soluble in HFIP, TFA, formic acid, and sulfuric acid. The limited solubility of the isolated polymers in common organic solvents made accurate determination of molecular weights by solution methods such as GPC very difficult. Hence, viscosity measurements in dichloroacetic acid were performed. Table 2 summarizes the polymerization results. The inherent viscosities vary from 0.11 for **P2** to 0.21 for **P5**. These values are very similar to viscosities obtained for poly(AlaGly) and related silklike polymers in dichloroacetic acid.[23b,c]

In our effort to obtain as much information as possible on the polymers, we subjected **P1** and **P2** to MALDI-TOF mass spectrometric analyses.[24] It must be pointed out that although MALDI-TOF MS has been shown to provide reliable MW averages for polymers with narrow MW distributions (polydispersity index, PDI, ≤1.20), it has also been found to be less reliable for polymers having high PDI as is usually the case for step-growth polymers. It was, therefore, not too surprising that the MALDI spectrum of **P1**, using either indoleacrylic acid or 3,5-dimethoxy-4-hydroxy-*trans*-cinnamic acid as matrix on a Lasermat 2000, showed a series of peaks up to *m*/*z* of only 7000 (ca. DP = 18), while that of **P2** showed peaks up to only *m*/*z* ~4,500 (ca. DP = 4). It appears that with the particular instrumental setup available to us, any higher molecular weight fractions present in the mixture were not adequately desorbed. The results are, however, in qualitative agreement with the trend in the viscosity data in that **P2** gave the lower viscosity. The methanol-soluble fraction from the synthesis of **P2** was also analyzed with MALDI in order to determine if cyclization was a complicating factor during the polymerization. The spectrum showed a large peak at *m*/*z* 1452.6. FABMS analysis of the same sample gave the MW as 1455.59, consistent with the linear unimer shown in Chart 2 (exact mass = 1454.43). Hence, under the particular interfacial polymerization conditions used, there is no evidence for appreciable formation of cyclic oligomers.

Solution Polymerization. The solution polymerizations of TFA salts of oligopeptides **18a′**−**d** were performed inside a drybox under nitrogen atmosphere at 25 °C using NMP (containing LiCl at 5% by weight) as solvent and diacid chloride **2** in the presence of diisopropylethylamine (Scheme 12). The polymerization conditions and results are summarized in Table 3. The polymers formed in moderate yields (39−67%, unoptimized). Inherent viscosities obtained in dichloroacetic acid varied from 0.14 to 0.20 g/dL, which are similar to

Scheme 12

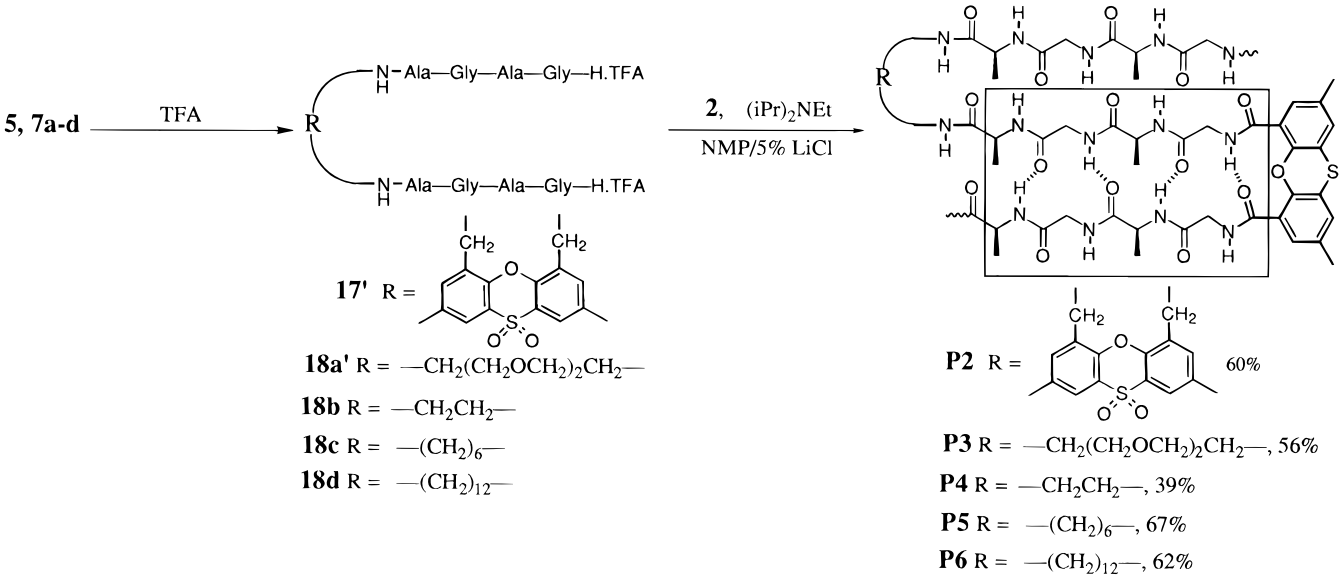

Chart 2

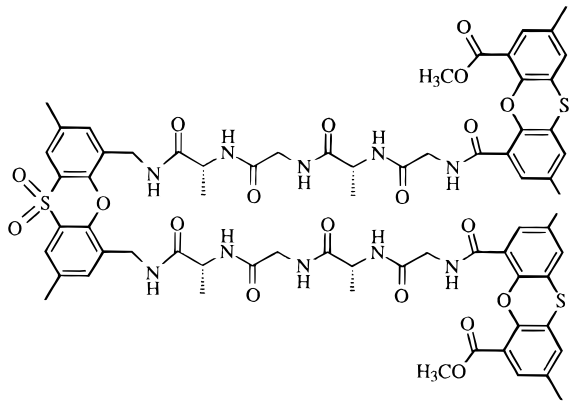

Table 3. Polyamides P2−P6 Prepared via Solution Polymerization[a]

polymer	[mon] (M)	yield (%)	M_n[b] (GPC)	M_w[b] (GPC)	DP[d]	η_{inh}[c] (dL/g)
P2	0.14	60	19 100	39 700	17	0.16
P4	0.20	39	17 400	26 900	24	0.14
P5	0.18	67	20 200	36 200	22	0.17
P6	0.16	62	22 400	35 600	23	0.17
P3	0.18	56	20 600	38 400	22	0.20

[a] Polymerizations were carried out in 5% LiCl/NMP at room temperature under an atmosphere of N_2. [b] Molecular weights versus polystyrene standards were estimated in 0.02 M LiCl in DMAC by GPC. [c] Inherent viscosities measured in dichloroacetic acid at 25.0 °C and a concentration of 0.5 g/dL. [d] Degree of polymerization from M_n.

those obtained for the interfacial polymers. Since the polymers contain flexible segments and reverse turn mimics designed to fold the chains, the overall rigidity of the polymers would not be expected to be high, especially if the chains adopt the expected folded conformations. Hence, the viscosity values do not necessarily indicate very low molecular weights. In order to obtain further molecular weight information, GPC was performed *in situ* using 0.02 M LiCl in DMAC as eluent and polystyrene standards. Since we have found that the polymers once isolated were difficult to redissolve, known aliquots of the reaction mixture were taken, diluted to the appropriate concentrations, and injected directly onto the GPC columns. Consequently, the GPC traces showed the presence of some cyclic oligomers (not seen in the interfacial method) since no purification was performed. For example, FABMS analyses of **P4** gave *m/z* ratios at 853.2 and 1705.5 corresponding to cyclic unimer and cyclic dimer, respectively, while FABMS of **P5** gave a cyclic unimer peak at 909.1. However, the use of GPC allowed us to estimate the molecular weights of the polymers. Weight-average molecular weights (M_w) which are less sensitive to the presence of oligomers varied from 27 000 for **P4** to about 40 000 for **P2**. From the number-average molecular weight (M_n) values, approximate average DP's were estimated (Table 3) to be 17 (**P2**), 22 (**P3**), 20 (**P4**), 22 (**P5**), and 23 (**P6**). These are taken as lower MW limits since M_n is influenced by the presence of oligomers. The above values are approximate since polystyrene may not represent the best standard for these polymers.

Solid State Properties. 1. Conformations of the Peptide Chains. The biomolecular Lego set concept requires that the predominant conformations of the prefabricated building blocks be retained in the corresponding polymers. We have already conclusively established that the phenoxathiin template induced formation of parallel β-sheets in the appropriate building blocks. Since the polymers were insoluble in solvents used for the studies of the building blocks, we employed resolution-enhanced solid state FTIR to probe for formation of secondary structures in both the building blocks and the polymers. The amide I carbonyl stretching region is highly sensitive to the secondary structure of polypeptides and proteins in solution and in the solid state.[25,26] In general, the amide I carbonyl stretching frequencies in random coil conformations occur at 1656 cm^{-1}, α-helices at 1650 cm^{-1}, antiparallel pleated β-sheets at 1632 cm^{-1} (strong) accompanied by a weak band at ca. 1685 cm^{-1} and parallel β-sheets at ca. 1630 cm^{-1} (strong) accompanied by a weaker band at ca. 1645 cm^{-1}.[25a,26a−d] Because the 1630 cm^{-1} absorption is common to both types of sheets, the one at 1645 cm^{-1} becomes the best diagnostic band for a parallel β-sheet.

The solid state FTIR spectra of monomer **5** and the corresponding hybrid polymer **P2** are shown in Figure 5. The sequence GAGA has been shown to have a high tendency to form antiparallel β-sheets in the solid state.[23d,26d] However, the peptide strands attached to

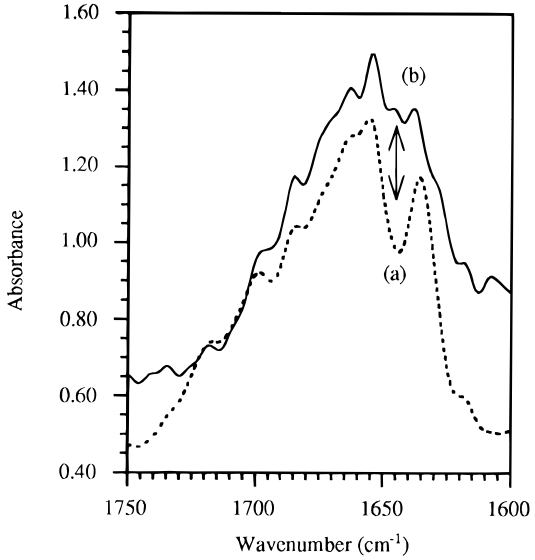

Figure 5. Resolution-enhanced solid state FTIR spectra (KBr, 2.0 cm^{-1} resolution, room temperature): (a) **5**; (b) **P2**. Spectra were recorded on a Perkin Elmer 16PC spectrometer.

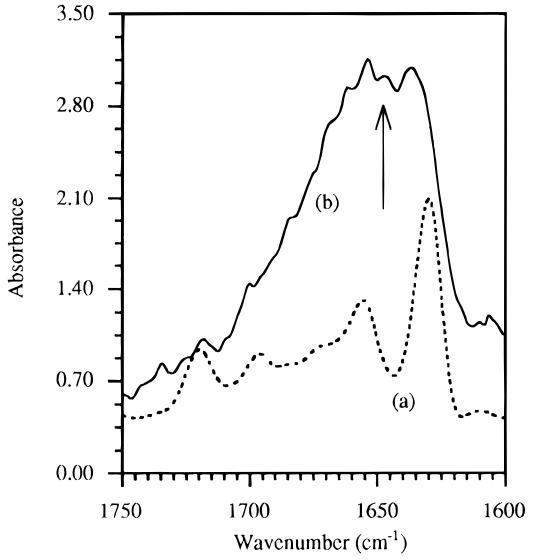

Figure 6. Resolution-enhanced solid state FTIR spectra (KBr, 2.0 cm^{-1} resolution, room temperature): (a) **7a**; (b) **P3**, expanded 8×. Spectra were recorded on a Perkin Elmer 16PC spectrometer.

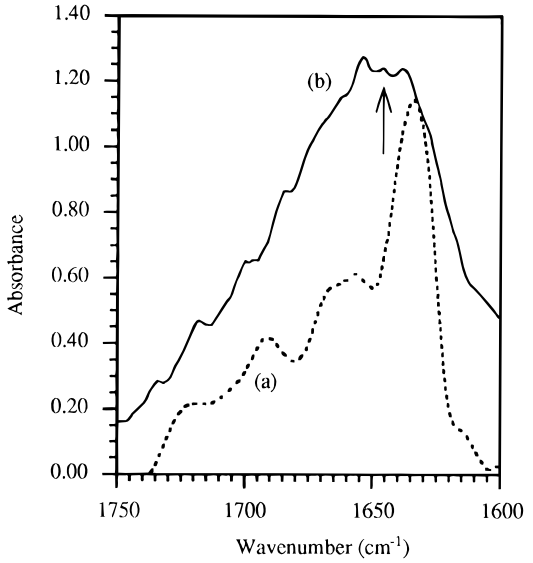

Figure 7. Resolution-enhanced solid state FTIR spectra (KBr, 2.0 cm^{-1} resolution, room temperature): (a) **7b**; (b) **P4** expanded 2×. Spectra were recorded on a Perkin Elmer 16PC spectrometer.

the phenoxathiin unit are expected to align in a parallel fashion. We have shown through model studies that the same sequence, when attached to a flexible linker, did not lead to formation of parallel β-sheet (*vide infra*). Building block **5** (Figure 5a) gave a strong amide I absorption at 1657 cm^{-1} with a shoulder at 1661 cm^{-1} corresponding to a random coil conformation and a strong absorbance at 1634 cm^{-1} and weak ones at 1686 and 1702 cm^{-1} corresponding to antiparallel β-sheets as expected for the GAGA sequence. No evidence for parallel sheet was observed as indicated by the absence of a band at 1645 cm^{-1}. This also suggests that, unlike the basic phenoxathiin unit, the sulfoxide derivative does not template the formation of parallel β-sheets even in a solid state. As noted earlier, this structural motif, due to the presence of the sulfoxide group, is less likely to adopt the near planar conformation required for optimum nucleation of stable hydrogen bond formation.[7b-d] In contrast, the solid state FTIR spectrum of the corresponding polymer **P2** (Figure 5b) showed absorption bands at 1635 and 1645 cm^{-1} indicating the presence of a parallel β-sheet. Random coil conformation bands at 1662 and 1656 cm^{-1} and antiparallel β-sheet bands at 1635 and 1685 cm^{-1} seen for **5** were also observed for **P2**. Hence, the microstructure of **P2** contains the expected mixture of parallel and antiparallel β-sheets and random conformations in the solid state. The parallel sheets are attributed to intrachain hydrogen bonding induced by the phenoxathiin unit serving as a hairpin turn mimic (boxed region of the structures), while the antiparallel sheets are due to interchain hydrogen bonding. In comparison, the solid state FTIR of nylon-6,6 shows bands at ca. 1640 cm^{-1} consistent with the existence of extended conformations where only interchain and no intrachain interactions exist.[26d] Hence, the observed antiparallel absorptions for **P2** might be due to interchain interactions as in the case of nylon and building block **5**. The peptide segments in the vicinity of the phenoxathiin sulfoxide might be more random than ordered which would explain the absorptions at 1662 and 1656 cm^{-1}.

The solid state FTIR spectra for **7a** and polymer **P3** are shown in Figure 6. The spectrum of monomer **7a** (Figure 6a) showed a mixture of antiparallel β-sheet (1630 and 1684 cm^{-1}) and random coil (1656 cm^{-1}) with no evidence for formation of parallel β-sheet. This is consistent with the earlier observation that replacement of the rigid template with a flexible chain resulted in almost complete absence of intermolecular hydrogen bond formation. In contrast, the solid state FTIR spectrum of **P3** (Figure 6b) is virtually identical with those of **P2** (Figure 5b) and silk fibroin.[23b-d,26d] The amide I band at 1648 cm^{-1} indicates that polymer **P3**, like **P2**, forms parallel β-sheets in the solid state. The FTIR spectra of **P4** and **P5** and their analogous building blocks (Figures 7 and 8) also confirm the above deductions. Thus, whereas the flexible building blocks (**18b**,**c**) showed no parallel sheet formation, the polymers **P4** and **P5** showed pairs of bands at 1630 and 1644 cm^{-1}, and at 1634 and 1645 cm^{-1} respectively, corresponding to parallel β-sheets.

To shed more light on the microstructure of the polymers, octapeptides **19** and **20** (Chart 3), which model the expected parallel β-sheet domain of the

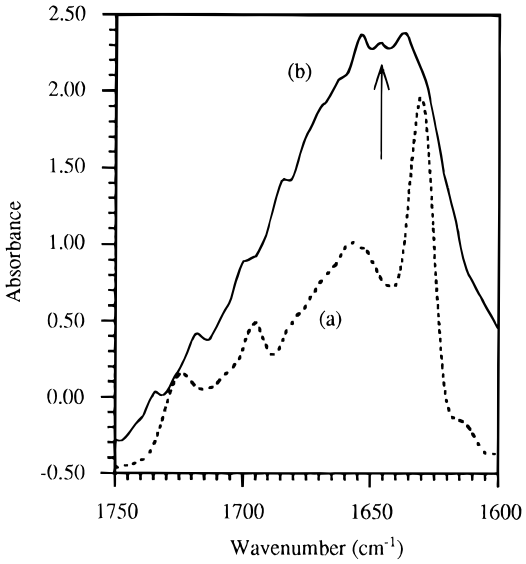

Figure 8. Resolution-enhanced solid state FTIR spectra (KBr, 2.0 cm^{-1} resolution, room temperature): (a) **7c**; (b) **P5**, expanded 4x. Spectra were recorded on a Perkin Elmer 16PC spectrometer.

Chart 3

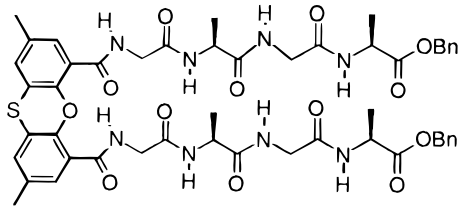

19

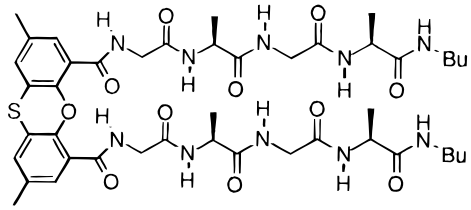

20

polymers, were prepared and studied by FTIR spectroscopy. The solid state FTIR spectrum of **19** (see the Supporting Information) was very similar to those of **P2** and **P3** showing a mixture of parallel β-sheet (1648 cm^{-1}), intersheet antiparallel β-sheet (1637 and 1684 cm^{-1}), and random conformations (1654 and 1662 cm^{-1}). Figure 9 shows the raw (a), resolution-enhanced (b) and second-derivative (c) FTIR spectra of **20**. Clearly, **20** exists predominantly in the parallel β-sheet conformation as evidenced by the strong absorptions at 1637 and 1649 cm^{-1}. Absorptions normally attributed to antiparallel and random conformations are virtually absent. The strong band at 1666 cm^{-1} is attributed to the aromatic carbonyl group. This band was observed in the spectra of phenoxathiin derivatives we have studied whether or not they contained peptides. Thus, **20** provides an authentic example of a parallel β-sheet-containing polypeptide. Previous studies to demonstrate the formation of parallel sheets involved proteins known to contain predominantly parallel β-sheets such as triosephosphate isomerase and flavodoxin and those containing mixed β-strands such as carboxypeptidase A.[26e] However, the proteins contain other conformations whose amide I bands complicate unambiguous assign-

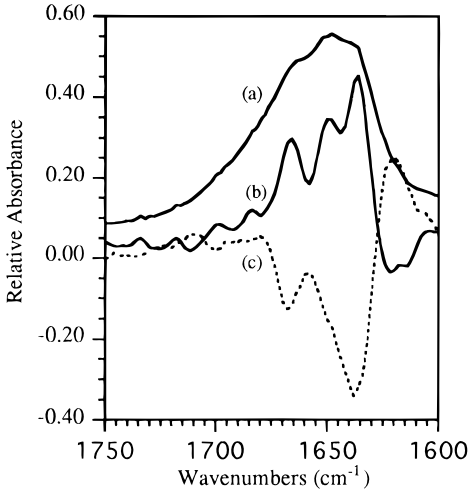

Figure 9. Raw, resolution-enhanced, and second-derivative FTIR spectra (KBr, 4.0 cm^{-1} resolution, room temperature) of **20**. Spectra were recorded on a Perkin Elmer 16PC spectrometer.

Table 4. FTIR Amide I Stretching Frequencies from Resolution-Enhanced Spectra of Polyamides P2−P6 and Their Corresponding Building Blocks 5 and 7a−d[a]

	stretching frequencies (cm^{-1})
	Hybrid Polymers
silk fibroin	1632, 1657, 1701
poly(AlaGly)[b]	1630, 1702
P2	1635, 1645, 1656, 1662, 1686, 1698
P4	1631, 1644, 1650, 1669, 1682, 1696
P5	1634, 1645 (sh), 1654, 1666, 1685, 1699
P6	1633, 1643 (sh), 1650, 1662, 1666, 1681, 1694
P3	1631, 1648, 1658 (sh), 1664, 1669, 1686, 1697
	Building Blocks
20	1637, 1649, 1666, 1684, 1699
5	1634, 1657, 1661 (sh), 1675 (sh), 1686, 1702, 1720
7b	1635, 1658, 1664, 1691, 1722
7c	1636, 1656, 1665 (sh), 1672 (sh), 1686, 1700, 1722
7d	1630, 1655, 1671, 1684, 1697, 1723
7a	1630, 1656, 1671, 1684, 1696, 1720

[a] Samples prepared as KBr pellets; 50 scans taken at a resolution of 4.0 cm^{-1}; sh = shoulder. [b] Spectra obtained from oriented films. Taken from Fraser, R. D. B.; MacRae, T. P.; Stewart, F. H. C.; Suzuki, E. *J. Mol. Biol.* **1965**, *11*, 706−712.

ments. More recent studies utilized the tripeptide $(Ala)_3$ that crystallized in both parallel and antiparallel conformations.[27]

The stretching frequencies of the amide I absorptions for the polymers prepared in solution were, to a large extent, the same as observed for the polymers prepared by interfacial techniques. The major differences were in the relative intensities of the absorption bands of interest. Representative FTIR spectra are shown in Figures 10 (**P2**), 11 (**P3**), and 12 (**P4**). The rest are given in the Supporting Information. The bands attributed to parallel β-sheets were more clearly resolved and stronger than those observed for the interfacial polymers. The peak assignments were accomplished through the use of a combination of resolution-enhanced and second-derivative spectra for each polymer. Several observations can be made as follows: The bands between 1640 and 1650 cm^{-1} are stronger for **P4**−**P6** than for **P2** and **P3**. **P4**−**P6** differ only in the length of the hydrocarbon spacers, and accordingly, their spectra were very similar. The higher flexibility of **P2** and the nonplanar nature of the linker in **P3** might partly

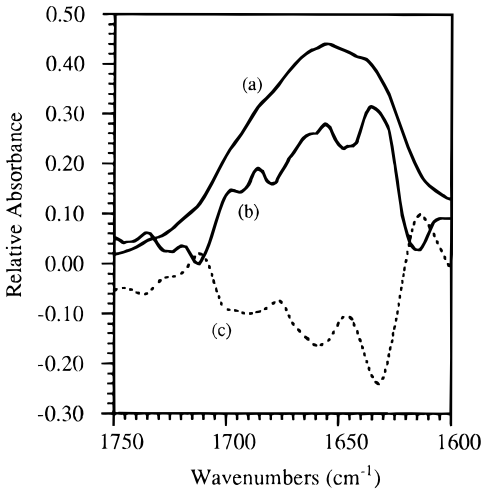

Figure 10. Raw (a), resolution-enhanced (b), and second-derivative (c) FTIR spectra (KBr, 4.0 cm^{-1} resolution, room temperature) of **P2**. Spectra were recorded on a Perkin Elmer 16PC spectrometer.

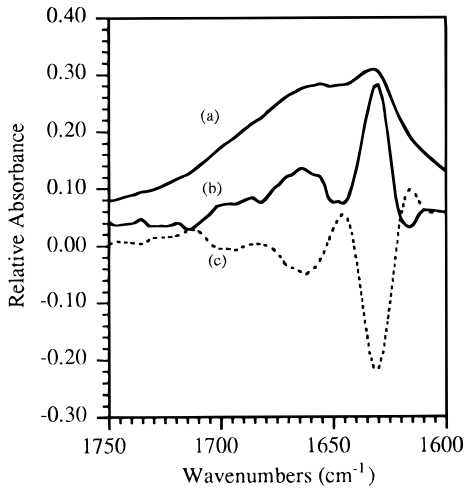

Figure 11. Raw (a), resolution-enhanced (b), and second-derivative (c) FTIR spectra (KBr, 4.0 cm^{-1} resolution, room temperature) of **P3**. Spectra were recorded on a Perkin Elmer 16PC spectrometer.

account for the difference. Another possible factor is the amount of water that might be incorporated into each polymer during isolation. It has been observed that parallel β-sheets tend to prefer a water-free environment which is consistent with the observation that parallel β-sheets present in proteins tend to be buried within the protein protected from interactions with water solvent molecules.[27a] In our case, **P2** and **P3**, due to the higher heteroatom content in their linkers compared to **P4**−**P6**, might absorb more water molecules into their structures during isolation and handling. If these tentative generalizations hold, they will suggest that the properties of the polymers can be influenced by the types of β-sheet structures incorporated. Overall, these solid state FTIR results are consistent with our results of conformational studies in solution, in that a rigid template is essential for the folding of the chains into parallel β-sheets.

2. Thermal Properties. The thermal analyses data for the polymers are summarized in Table 5. For comparison the thermal properties of nylon-6,6, nylon-6, and *B. mori* silk fibroin are included.[12a,15b,28] Nylon-6,6 has a glass transition temperature (T_g) of 50 °C and a melting temperature (T_m) of 265 °C.[15b] **P1** shows a

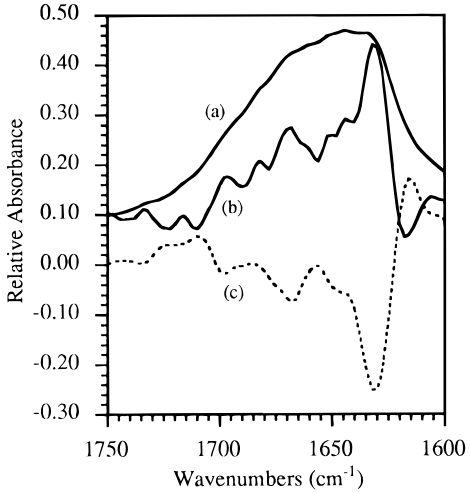

Figure 12. Raw (a), resolution-enhanced (b), and second-derivative (c) FTIR spectra (KBr, 4.0 cm^{-1} resolution, room temperature) of **P4**. Spectra were recorded on a Perkin Elmer 16PC spectrometer.

Table 5. Thermal Properties of Polyamides P1−P6 and Model Compound 20[a]

polymer	T_g (°C) (DSC) solution	T_g (°C) (DSC) interfacial	T_m (°C) (DSC)	$T_{d,onset}$ (°C) (TGA)
nylon-6,6[b]	50		265	
nylon-6[b]	52		223	
P1[c]		149		368
silk fibroin (r)[d]	175			250
P2[c]	204	192		313
P4	186	168		293
P5	168	160		293
P3	156	149		278
P6[c]	148			290
20	132			310

[a] Performed under an N_2 atmosphere. [b] Taken from *Polymer Handbook*, 3rd ed.; Bandrup, J., Immergut, E. H., Eds.; Wiley-Interscience: New York, 1989. [c] DSC heating rate = 10 °C/min. [d] Silk fibroin in random coil conformation; heating rate of DSC 8 °C/min.

T_g of 149 °C; no T_m was observed below the onset decomposition temperature, T_d. This is consistent with nylon-6,6 being more flexible than **P1**. Amorphous silk fibroin shows a T_g at 175 °C and crystallizes in the β-form above 180 °C.[12a] In comparison, these synthetic silk analogs showed T_g's that were dependent on the type of organic linker and, surprisingly, the method of polymerization. Although unexpected, this is in agreement with the FTIR results, in that the parallel sheet content is higher for the solution polymers. In general, the T_g's decreased in the following order: **P2** > **P4** > **P5** > **P3** > **P6**, which roughly paralleled increasing flexibility of the linkers. The polymers prepared by solution method showed higher T_g's than did the corresponding ones made by interfacial polymerization. The dependence of polymer morphologies on synthesis and isolation procedures has been observed for many polymers, especially aromatic ones, such as Kevlar.[23a] The hybrid polymers appeared to be more thermally stable than silk fibroin as evidenced by their higher T_d's (*T*GA). The results of the structure−property relationship studies of the silk-based polymers reported herein demonstrate the advantage of using a modular synthetic method to prepare bioinspired polymers. By a judicious combination of peptide segments with nonnatural segments, we have been able to influence the dependence of properties on structure. To obtain similar variation

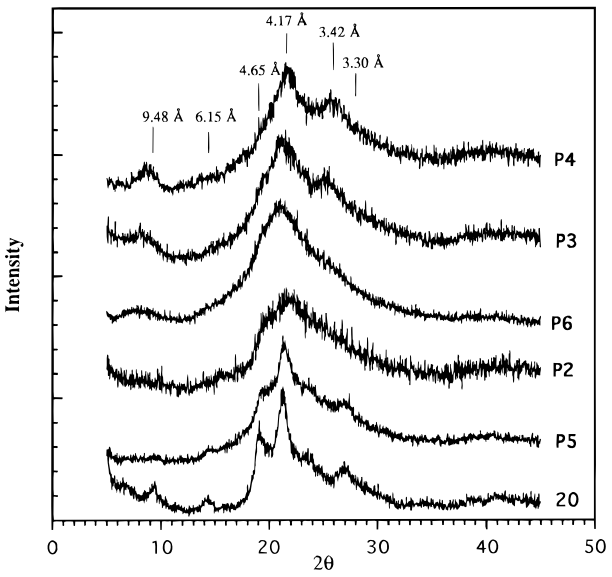

Figure 13. X-ray powder diffraction spectra of **P2**−**P6** and **20**; wavelength, $\lambda = 0.154$ nm (1.5 kW, Cu Kα).

in property as a function of structure in natural silks one would have to resort to different natural sources.

Powder X-ray Diffraction Studies. Figure 13 shows the powder diffraction patterns for the unoriented polymers and the model octapeptide **20** which indicate that all the "as-made" polymers are semicrystalline. The model compound **20** is the most crystalline and shows a spectrum resembling that of **P5**. The spectra for **P3**, **P4**, and **P6** resemble those obtained for oriented silklike fibers, such as *Adenovirus* constructs and other genetically engineered silklike polymers.[12b] Efforts are underway to prepare oriented fibers in order for the spectra to be indexed on appropriate space groups. Further work, such as morphological and mechanical properties measurements, is required to fully understand the structure−property relations observed for these polymers.

Summary and Conclusions

The results of our spectroscopic studies show that phenoxathiin is an effective nucleating agent for hydrogen bonding crucial for β-sheet formation. Unlike the divergent dibenzofuran template,[7e−h] the rigid phenoxathiin unit does not require insertion of spacers between the aromatic nucleus and the first amide groups. Even esters, such as the ester amide **10**, exist almost exclusively in an intramolecularly hydrogen-bonded conformation. The low and similar $-\Delta\delta/\Delta T$ values for both hydrogen-bonded and non-hydrogen-bonded amide NH's in dilute CD_2Cl_2 solutions are attributed to steric shielding of the amide protons closest to the phenoxathiin unit and to equilibrating degenerate conformations. The variable temperature studies in DMSO-d_6 provide more conclusive evidence for the existence of β-sheet conformation. Comparative FTIR spectroscopic studies of propagating models **13** and **15** provide conclusive evidence for the necessity of using a rigid template since replacing the phenoxathiin derivative with a flexible hydrocarbon chain results in a substantial loss of intramolecular hydrogen bonding. The results are further substantiated by titration of dilute CD_2Cl_2 solutions of the peptides with DMSO-d_6 during which the chemical shifts of the hydrogen-bonded amide NH's are much less affected than those of the free NH's.

We have demonstrated that the biomolecular Lego set modular approach to the synthesis of peptide-based polymers where prefabricated building blocks are linked block by block is an appropriate technique for polymer architecture control. Solid state FTIR revealed that the expected parallel β-sheets were retained in the polymer solely due to the presence of the rigid phenoxathiin template which also suggests that folding of the chains occurs in the vicinity of the template. We have shown that conformationally flexible units do not induce sheet formation in short chain peptides. Hence, their incorporation into polymers provides mostly random coils and interchain antiparallel hydrogen bonding. The nature of the β-sheet domains was confirmed through the study of model octapeptides **19** and **20**. DSC and TGA studies revealed that as the flexibility of the linkers decreases, T_g and onset decomposition temperatures also decrease. Surprisingly, the polymerization method (interfacial versus solution) has some effect on the T_g's. The properties of the polymers compare well with those of silk and nylon. X-ray diffraction analysis suggests that the polymers are semicrystalline. Optimization of polymerization conditions, detailed microstructure characterization, efforts to orient the chains and induce crystallization, incorporation of hydrophilic and/or surface active functional groups on the folds, and application to other monomers are in progress.

Experimental Details

General. All glassware were oven-dried where appropriate and cooled under nitrogen. Ethereal solvents were distilled from sodium/benzophenone ketyl. Diisopropylethylamine and *N*-methylpyrrolidinone (NMP) were distilled from CaH_2 onto 4 Å molecular sieves and stored under N_2 in a drybox. LiCl was dried under high vacuum at 120 °C prior to use. Melting points were determined using a capillary melting point apparatus and are uncorrected. Proton NMR spectra were recorded on a Varian XL200, Varian VXR 400S, or Varian Unity 500 spectrometer. ^{13}C NMR spectra were recorded on a Varian VXR 400S spectrometer. IR spectra were recorded on a Perkin Elmer 16PC FTIR spectrometer. Solid state IR samples were prepared as KBr pellets (1−2% by weight), and spectra were obtained with 50 scans at a resolution of 4.0 cm^{-1} unless otherwise noted. Fast atom bombardment (FAB) and electron impact (EI) mass spectral data were obtained from the University of Illinois Mass Spectrometry Laboratory. Elemental analyses were performed by Oneida Research Services, Inc. or Texas Analytical Laboratories, Inc. Variable temperature and solvent titration studies were carried out on VXR 400S and/or Varian Unity 500 spectrometers. Solvent titrations were done at 23.5 °C by addition of small volumes of DMSO-d_6 successively to the peptide dissolved in 1 mL of CD_2Cl_2. The spectra for determination of temperature gradients were recorded between 193 and 293 K in CD_2Cl_2 or 303−373 K in DMSO-d_6 in increments of 10 or 20 K. Solubility tests of the polymers were carried out at 1 mg/mL concentration. Inherent viscosity measurements were determined in dichloroacetic acid (DCA) solutions at a concentration of 0.5 g/dL with a Cannon-Ubbeholde C1 C866 viscometer placed in a water bath thermostated at 25.0 ± 0.1 °C. Gel permeation chromatography (GPC) analyses were carried out with a Waters 510 HPLC pump and a Hewlett Packard series 1050 UV detector ($\lambda = 270$ nm). One GPC column, PL Gel Mixed C (5 μm), was used with 0.02 M LiCl in *N*,*N*-dimethylacetamide (DMAC) as the eluent at 40 °C and a flow rate of 1.0 mL/min. Molecular weights were estimated using narrow molecular weight polystyrene standards. Powder X-ray diffraction studies were performed on a Scintag theta-theta X-ray diffractometer. The instrument was equipped with a 1.5 kW Cu Kα tube which emits X-ray radiation at a wavelength of 0.154 nm. Thermogravimetric analysis (TGA) and differential scanning calorimetry (DSC) were performed on a Seiko 5200 thermal analysis system with TGA/DTA 220 and DSC 220C units. TGA

runs were performed under a positive flow of nitrogen at a heating rate of 20 °C/min. DSC runs were also performed under a positive flow or nitrogen at a heating/cooling rate of 10 °C/min; T_g's were recorded from the second heating cycles.

2,8-Dimethylphenoxathiin-4,6-dicarboxylic Acid (1). In a 250 mL round-bottom flask equipped with a stirring bar and a rubber septum was dissolved 2,8-dimethylphenoxathiin (3.00 g, 13.1 mmol) in THF (100 mL) under N_2. The pale yellow solution was cooled to −40 °C, and *n*-BuLi (13.0 mL, 2.5 M in hexane) was added dropwise via syringe. The solution became amber in color upon this addition. The solution was stirred for 1 h at −40 °C, allowed to warm to room temperature, and stirred for an additional 5 h. The reaction mixture was injected via syringe onto solid CO_2 in a 500 mL round-bottom flask. The excess CO_2 was allowed to evaporate and the mixture allowed to stand overnight. The yellow solution was concentrated via rotary evaporation and taken up in 1 N NaOH (50 mL)/H_2O (50 mL). The crude material was precipitated with HCl, filtered, and washed with H_2O. The partially dried filter cake was taken up in hot MeOH and filtered (repeated 1×). The combined solids were dried *in vacuo* giving 2.49 g (60%) of **1**. This was further purified by recrystallization from 2-butanone: R_f 0.28 (10% MeOH in methylene chloride); mp 286−288 °C. MS (EI, 70 eV): *m/z* 316 (M^+, 100), 272 (18), 239 (15). HRMS (EI): calcd for $C_{16}H_{12}O_5S$, 316.04 (M^+); found, 316.04.

2,8-Dimethylphenoxathiin-4,6-dicarbonyl Chloride (2). To a 250 mL round-bottom flask equipped with a magnetic stirring bar and a gas-inlet adapter were added **1** (2.04 g, 6.45 mmol) and oxalyl chloride (15 mL) under N_2. To the cloudy mixture was added 5 drops of DMF whereupon vigorous bubbling occurred. The reaction mixture became clear as it was stirred for 3 h at room temperature. The solution was concentrated via rotary evaporation, and CH_2Cl_2 (10 mL) was added. The solution was again concentrated (repeated 2×). The dried yellow solid was recrystallized from hexanes under N_2 to yield 1.83 g of yellow needles (80%): mp 133.0−134.5 °C. HRMS (EI): calcd for $C_{16}H_{10}Cl_2O_3S$, 351.9728; found 351.9725 (M^+). Anal. Calcd for $C_{16}H_{10}Cl_2O_3S$: C, 54.41; H, 2.85; Cl, 20.07; S, 9.08. Found: C, 54.65; H, 2.78.

2,8-Dimethylphenoxathiin-4-carboxylic Acid (3). (A) Synthesis of the Intermediate 2,8-Dimethylphenoxathiin-4-carboxylic Acid Methyl Ester. To a dry 100 mL round-bottom flask equipped with a magnetic stirring bar and a rubber septum was added 2,8-dimethylphenoxathiin (866 mg, 3.79 mmol). The flask was evacuated and back-flushed with N_2 three times. Freshly distilled THF (50 mL) and TMEDA (0.80 mL, 5.3 mmol) were added to the flask via a syringe. The solution was cooled to −30 °C, and BuLi (3.00 mL, 1.4 M in pentane, 4.20 mmol) was added dropwise using a syringe. The mixture was stirred at −30 °C under N_2 for 1.5 h. Dry CO_2 gas was bubbled through the mixture for 10 min, and the mixture was allowed to warm to room temperature. The mixture was concentrated to dryness, a condenser was attached, and a solution of H_2SO_4 (5 mL) in methanol (50 mL) was added. The reaction mixture was refluxed for 3 h, cooled, poured into a beaker containing saturated aqueous $NaHCO_3$, and extracted with ethyl acetate. The crude mixture was dried over $MgSO_4$, filtered, and concentrated to give a light brown oil (1.14 g) which was then loaded onto a column of silica gel. The mixture was subjected to gradient elution with petroleum ether and ethyl acetate. The desired product, 2,8-dimethylphenoxathiin-4-carboxylic acid methyl ester, eluted from the column as an oil (905 mg, 69%): R_f 0.38 (4:1 hexane/EtOAc, v/v). ^{1}H NMR (200 MHz, $CDCl_3$): δ 7.39 (s, 1H, Phen-H), 7.06 (s, 1H, Phen-H), 6.85−7.02 (m, 3H, Phen-H), 3.94 (s, 3H, ester-CH_3), 2.26 (s, 6H, Phen-CH_3).

(B) Hydrolysis of the Methyl Ester To Give 3. To a stirred suspension of potassium *tert*-butoxide (5.40 g, 13.0 mmol) in THF (100 mL) was added H_2O (0.20 mL, 11 mmol) via a syringe. After 10 min of stirring the methyl ester from part A (1.06 g, 3.70 mmol) was added. The mixture was stirred overnight at 25 °C. Water was added until two clear layers formed. The aqueous layer was acidified with HCl and extracted with CH_2Cl_2. The organic layer was dried over $MgSO_4$, filtered, and concentrated to a yellow solid. Trituration with ether gave pure monoacid **3** (0.94 g, 93%): R_f 0.30 (5% MeOH in CH_2Cl_2); mp 181−183 °C. HRMS (EI): calcd for $C_{15}H_{12}O_3S$, 272.05 (M^+); found, 272.05.

Synthesis of Octapeptide 5. To a 200 mL round-bottom flask equipped with a magnetic stirring bar and a stopper were added BOC-GlyAlaGlyAla-OH (967 mg, 2.58 mmol), HOBT·H_2O (406 mg, 2.65 mmol), and DMF (100 mL). The stirred mixture was cooled to 0 °C, and DCC (532 mg, 2.58 mmol) was added. After 15 min of stirring 2,8-dimethyl-4,6-bis(aminomethyl)-phenoxathiin 10,10-dioxide (**4**; 400 mg, 1.26 mmol) was added, and the cooling bath was removed. The mixture was allowed to stir overnight and then evaporated to give a solid. Purification was accomplished by continuous Soxhlet extraction with acetone for 1 day to yield 827 mg of a white solid (**5**, 64%): R_f 0.19 (10% MeOH in CH_2Cl_2); mp 195 °C dec; $[\alpha]^{25}_D = -7.0°$ (c = 1, DMSO). HRMS (FAB): calcd for $C_{46}H_{67}N_{10}O_{15}S$, 1031.45 ($MH^+$); found, 1031.45. Anal. Calcd for $C_{46}H_{66}N_{10}O_{15}S$: C, 53.58; H, 6.45; N, 13.58. Found: C, 53.50; H, 6.43; N, 13.38.

2,2′-(Ethylenedioxy)bis(ethylamine)-Containing Octapeptide 7a. The procedure for **5** above was followed using BOC-GAGA-OH (5.20 g, 13.9 mmol), HOBT·H_2O (2.23 g, 14.6 mmol), DMF (100 mL), DCC (2.87 g, 13.9 mmol), and 2,2′-(ethylenedioxy)bis(ethylamine) (970 μL, 6.64 mmol). Purification was accomplished by continuous Soxhlet extraction of the pulverized solid with acetone for 4 days to yield 4.66 g of a white solid (**7a**, 81%): R_f 0.0 (10% MeOH in CH_2Cl_2); mp 229 °C dec; $[\alpha]^{25}_D = -12.0°$ (c = 1, DMSO-d_6). Anal. Calcd for $C_{36}H_{64}N_{10}O_{14}$: C, 50.22; H, 7.49; N, 16.27. Found: C, 50.50; H, 7.65; N, 16.26.

Ethylenediamine-Containing Octapeptide 7b. This was similarly prepared using BOC-GAGA-OH (3.20 g, 8.55 mmol), HOBT·H_2O (1.34 g, 8.76 mmol), DMF (100 mL), ethylenediamine (280 μL, 4.19 mmol), and DCC (1.87 g, 9.06 mmol): yield, 2.32 g (72%, white solid). $[\alpha]^{25}_D = -16.6°$ (c = 1, DMSO). HRMS (FAB): calcd for $C_{32}H_{57}N_{10}O_{12}$, 773.42 (MH^+); found, 773.42. Anal. Calcd for $C_{32}H_{56}N_{10}O_{12}$: C, 49.73; H, 7.30; N, 18.12. Found: C, 49.45; H, 7.16; N, 17.70.

Hexamethylenediamine-Containing Octapeptide 7c. The above procedure was followed replacing ethylenediamine with hexamethylenediamine to give **7c** in 72% yield: $[\alpha]^{25}_D = -14.5°$ (c = 1, DMSO). HRMS (FAB): calcd for $C_{36}H_{65}N_{10}O_{12}$, 829.48 (MH^+); found, 829.48. Anal. Calcd for $C_{36}H_{64}N_{10}O_{12}$: C, 52.16; H, 7.78; N, 16.90. Found: C, 52.38; H, 7.54; N, 16.69.

Synthesis of 1,12-Diaminododecane-Containing Octapeptide 7d. The same procedure was followed using BOC-GAGA-OH (4.87 g, 13.0 mmol), HOBT·H_2O (2.09 g, 13.6 mmol), DMF (100 mL), DCC (2.68 g, 13.0 mmol), and 1,12-diaminododecane (1.24 g, 6.19 mmol). The mixture was allowed to stir for 3 days and evaporated to give a solid. Purification by continuous Soxhlet extraction of the pulverized solid with acetone overnight gave 5.06 g of a white solid (99%). $[\alpha]^{25}_D = -13.0°$ (c = 1, DMSO). HRMS (FAB): calcd for $C_{42}H_{77}N_{10}O_{12}$, 913.57 (MH^+); found, 913.57. Anal. Calcd for $C_{42}H_{76}N_{10}O_{12}$: C, 55.25; H, 8.39; N, 15.34. Found: C, 55.11; H, 8.43; N, 15.31.

2,8-Dimethylphenoxathiin-4,6-dicarboxylic Acid Monobenzyl Ester (8). To a 200 mL round-bottom flask equipped with a magnetic stirring bar and a condenser were added **1** (2.35 g, 7.43 mmol), benzyl bromide (890 μL, 7.48 mmol), Et_3N (1.04 mL, 7.43 mmol), and distilled THF (100 mL). The mixture was allowed to reflux overnight and evaporated. The residue was taken up in CH_2Cl_2, washed with 5% aqueous citric acid (3×), dried over Na_2SO_4, filtered, and evaporated to give a solid. The impure material was purified by flash chromatography (silica gel, CH_2Cl_2 followed by 5% MeOH in CH_2Cl_2) to give **8** as a white powder (2.10 g, 70% yield): R_f 0.26 (2/1 hexane/EtOAc, v/v); mp 182.5−183.5 °C. HRMS (FAB): calcd for $C_{23}H_{19}O_5S$, 407.10 (MH^+); found, 407.09. Anal. Calcd for $C_{23}H_{18}O_5S$: C, 67.97; H, 4.46. Found: C, 68.01; H, 4.37.

***N,N′*-[(2,8-Dimethylphenoxathiin-4,6-diyl)dicarbonyl]-bis(*β*-alanine) Diethyl Ester (9).** To a 250 mL round-bottom flask equipped with a magnetic stirring bar and a rubber septum were added HCl·βAla-OEt (2.02 g, 13.2 mmol), Et_3N (1.84 mL, 13.2 mmol), 100 mL of distilled CH_2Cl_2, and DMF (10 mL) at 0 °C under N_2. To the neutralized mixture at 0 °C were **1** (2.09 g, 6.60 mmol), HOBT·H_2O (2.02 g, 13.2 mmol),

and DCC (2.78 g, 13.2 mmol). The resulting mixture was stirred for 10 min at 0 °C and overnight at room temperature. The urea byproduct (DCU) was filtered off and the filtrate evaporated. The residue was taken up in CH_2Cl_2 and refiltered to remove residual DCU. The organic phase was washed successively with 5% aqueous citric acid (2×) and 5% aqueous $NaHCO_3$ (2×), dried over Na_2SO_4, filtered, and evaporated to give 5.27 g of crude product. The crude product was purified by flash chromatography (silica gel, 5% MeOH in CH_2Cl_2) to give 3.12 g (92%) of **9** as an off-white solid: R_f 0.53 (5% MeOH in CH_2Cl_2); mp 153.5−155 °C. HRMS (FAB): calcd for $C_{26}H_{31}N_2O_7S$, 515.19 (MH^+); found, 515.19.

6-[[(Methoxycarbonyl)methyl]carbamoyl]-2,8-dimethylphenoxathiin-4-carboxylic Acid Benzyl Ester (10). To a 250 mL round-bottom flask were added **8** (1.05 g, 2.58 mmol), HCl·Gly-OMe (324 mg, 2.58 mmol), Et_3N (380 μL, 2.73 mmol), CH_2Cl_2 (75 mL). and DMF (5 mL). To the stirred mixture was added HOBT·H_2O (420 mg, 2.74 mmol). The reaction mixture was cooled to 0 °C and DCC (532 mg, 2.58 mmol) was added. The mixture was stirred for 15 min at 0 °C, and for 2 days at room temperature. The solvents were evaporated. The crude residue was taken up in CH_2Cl_2 and filtered to remove DCU. The organic layer was washed successively with 5% aqueous citric acid (3×), 5% aqueous $NaHCO_3$ (3×), and distilled H_2O (1×), dried over Na_2SO_4, filtered, and evaporated to give a pale yellow solid. The solid was taken up in hexanes/ethyl acetate (2:1, v/v) and filtered to remove residual DCU. The filtrate was concentrated and the procedure repeated with hexanes/EtOAc/CH_2Cl_2 (1:1:1, v/v/v) to give 1.14 g (93%) of **10** as an off-white solid. Analytically pure material was obtained after flash chromatography (silica gel, hexanes/EtOAc/CH_2Cl_2, 1:1:1, v/v/v): R_f 0.63 (1:1:1 hexanes/EtOAc/CH_2Cl_2, v/v/v); mp 142.5−143.7 °C. HRMS (FAB): calcd for $C_{26}H_{24}NO_6S$, 478.13 (MH^+); found, 478.13.

***N,N′*-[(2,8-Dimethylphenoxathiin-4,6-diyl)dicarbonyl]-bis(glycine) Dimethyl Ester (11).** The procedure for **9** was followed using a 50 mL round-bottom flask, HCl·Gly-OMe (564 mg, 4.49 mmol), Et_3N (650 μL, 4.66 mmol), distilled CH_2Cl_2 (30 mL), DMF (3 mL), **1** (678 mg, 2.14 mmol), HOBT·H_2O (714 mg, 4.66 mmol), and DCC (926 mg, 4.49 mmol). The crude product was purified by flash chromatography (silica gel, 3% MeOH in CH_2Cl_2) and subsequently washed with MeOH to give **11** in 73% yield (717 mg) as an off-white solid: R_f 0.34 (5% MeOH in CH_2Cl_2); mp 198.5−200.0 °C. HRMS (FAB): calcd for $C_{22}H_{23}N_2O_7S$, 459.12 (MH^+); found, 459.12. Anal. Calcd for $C_{22}H_{22}N_2O_7S$: C, 57.63; H, 4.84; N, 6.11. Found: C, 57.46; H, 4.93; N, 6.02.

***N*-[(2,8-Dimethylphenoxathiin-4-yl)carbonyl]-*β*-alanine Ethyl Ester (12).** The above procedure was followed using HCl·H_2N-*β*Ala-OEt (113 mg, 734 μmol), distilled CH_2Cl_2 (25 mL), DMF (2 mL), Et_3N (103 μL, 734 μmol), **3** (100 mg, 367 μmol), HOBT·H_2O (118 mg, 771 μmol), and DCC (151 g, 734 μmol). The crude product (224 mg) was purified by flash chromatography (silica gel, hexanes/EtOAc, 4:1, v/v) to give 102 mg (75%) of **12** as a white solid: R_f 0.50 (5% MeOH in CH_2Cl_2); mp 82−83.8 °C. HRMS (FAB): calcd for $C_{20}H_{22}NO_4S$, 372.13 (MH^+); found, 372.13. Anal. Calcd for $C_{20}H_{21}NO_4S$: C, 64.67; H, 5.70; N, 3.77. Found: C, 65.04; H, 5.85; N, 3.69.

***N,N′*-[(2,8-Dimethylphenoxathiin-4,6-diyl)dicarbonyl]-bis(glycyl-L-alanine) Dibenzyl Ester (13).** Similarly **13** was prepared using HCl·H_2N-Gly-Ala-OBn (379 mg, 1.39 mmol), distilled CH_2Cl_2 (20 mL), DMF (2 mL), Et_3N (200 μL, 1.43 mmol), **1** (200 mg, 632 μmol), HOBT·H_2O (242 mg, 1.58 mmol), and DCC (287 mg, 1.39 mmol). The impure material was purified by flash chromatography (silica gel, 5% MeOH in hexanes/EtOAc/CH_2Cl_2, 1:1:1, v/v/v) to give 309 mg (65% yield) of **13** as a white solid: R_f 0.30 (5% MeOH in hexanes/EtOAc/CH_2Cl_2, 1:1:1, v/v/v); mp 165.5−166.5 °C; $[\alpha]^{25}_D = +0.8°$ (c = 0.52, CH_2Cl_2). HRMS (FAB): calcd for $C_{40}H_{41}N_4O_9S$, 753.26 (MH^+); found, 753.26. Anal. Calcd for $C_{40}H_{40}N_4O_9S$: C, 63.82; H, 5.36; N, 7.44. Found: C, 64.04; H, 5.38; N, 7.39.

***N*-[(2,8-Dimethylphenoxathiin-4-yl)carbonyl]glycyl-L-alanine Benzyl Ester (14)**. The same procedure was followed using HCl·H_2N-Gly-Ala-OBn (36 mg, 132 μmol), CH_2Cl_2 (10 mL), DMF (10 mL), Et_3N (18 μL, 132 μmol), **11** (36 mg, 132 μmol), HOBT·H_2O (21 mg, 139 μmol), and DCC (27 mg, 132 μmol). The crude product (141 mg) was purified by flash chromatography (silica gel, 1% MeOH in CH_2Cl_2) to give the pure **14** (35 mg, 54% yield): R_f 0.29 (5% MeOH in CH_2Cl_2); mp 162.5−164 °C; $[\alpha]^{25}_D = -4.3°$ (c = 0.65, CH_2Cl_2). HRMS (FAB): calcd for $C_{27}H_{27}N_2O_5S$, 491.16 (MH^+); found, 491.16. Anal. Calcd for $C_{27}H_{26}N_2O_5S$: C, 66.11; H, 5.34; N, 5.71. Found: C, 66.08; H, 5.56; N, 5.58.

***N,N′*-(1,5-Pentanediyldicarbonyl)bis(glycyl-L-alanine) Dibenzyl Ester (15)**. The same procedure was followed using HCl·H_2N-GlyAla-OBn (266 mg, 975 μmol), CH_2Cl_2 (20 mL), DMF (5 mL), Et_3N (150 μL, 1.08 mmol), pimelic acid (72 mg, 450 μmol), HOBT·H_2O (172 mg, 1.12 mmol), and DCC (201 mg, 975 μmol). The crude product was purified by flash chromatography (silica gel, 10% MeOH in CH_2Cl_2) to give **15** as a white solid (222 mg, 83% yield): R_f 0.32 (10% MeOH in CH_2Cl_2); mp 145−146.5 °C; $[\alpha]^{25}_D = -43.2°$ (c = 1.10, MeOH). HRMS (FAB): calcd for $C_{31}H_{41}N_4O_8$, 597.29 (MH^+); found, 597.29.

Deprotection of 5 To Give 17. To a 50 mL round-bottomed flask were added **5** (190 mg, 185 μmol) and anhydrous TFA (10 mL). The solution was allowed to stir for 2 h at room temperature and evaporated. The oily residue was taken up in HCl (20 mL, 3.8 M in 1,4-dioxane) whereupon a white precipitate formed. This was filtered, and the solids were triturated with anhydrous diethyl ether to give 170 mg of the diamine·HCl **17** (102%):

2,2′-(Ethylenedioxy)bis(ethylamine) Octapeptide Hydrochloride (18a). The procedure for **17** was followed using **7a** (867 mg, 1.01 mmol) to give 1.16 g of **18** (57%).

***N,N′*-[(2,8-Dimethylphenoxathiin-4,6-diyl)dicarbonyl]-bis(glycyl-L-alanyl-glycyl-L-alanine) Dibenzyl Ester (19).** In a 50 mL round-bottom flask equipped with a magnetic stirring bar and a rubber septum were added HCl·H-GlyAla-GlyAla-OBn (104 mg, 259 μmol), distilled CH_2Cl_2 (10 mL), DMF (2 mL), and Et_3N (46 μL, 330 μmol) at 0 °C. The solution was allowed to stir for 15 min under N_2. To the neutralized solution were added **1** (41 mg, 130 μmol) and HOBT·H_2O (41 mg, 267 μmol). The solution was cooled to 0 °C, and DCC (53 mg, 260 μmol) was added. The reaction mixture was stirred at 0 °C for 10 min and overnight at room temperature, taken up in 10% MeOH/CH_2Cl_2, and filtered. The solids were saved. The filtrate was evaporated and the residue purified by flash chromatography (silica gel, 10% MeOH in CH_2Cl_2) to give 27 mg of a white solid which was shown to be the desired pure product (21%). The saved precipitate was washed successively with MeOH, H_2O, MeOH, and CH_2Cl_2 and dried to give pure **19** (45 mg, 34%): combined yield, 55%; R_f 0.28 (10% MeOH in CH_2Cl_2); mp 260−262.5 °C; $[\alpha]^{25}_D = -4.6°$ (c = 1, DMF). HRMS (FAB): calcd for $C_{50}H_{57}N_8O_{13}S$, 1009.38 (MH^+); found, 1009.38.

Synthesis of *N,N′*-[(2,8-Dimethylphenoxathiin-4,6-diyl)dicarbonyl]bis(glycyl-L-alanyl-glycyl-L-alanine)-*N*-butylamide (20). To a 250 mL round-bottom flask equipped as above were added BOC-GAGA-*n*-Bu (577 mg, 1.34 mmol) and TFA (5 mL) under N_2. The mixture was stirred for 3 h and evaporated. The dried solid residue was dissolved in DMF (50 mL) and treated at 0 °C with Et_3N (900 μL, 6.44 mmol), **1** (212 mg, 670 μmol), HOBT·H_2O (1.03 g, 6.70 mmol), and DCC (276 mg, 1.34 mmol). The resulting mixture was stirred for 3 days at room temperature and evaporated to give a solid which was pulverized and purified by continuous Soxhlet extraction with acetone overnight to yield 358 mg of a pale yellow solid (57%): $[\alpha]^{25}_D = -43.1°$ (c = 1.02, DCA). FABMS: 939.3 (MH^+). T_g 132 °C; $T_{d,onset}$ 310 °C.

Polymerizations. 1. Interfacial Polymerization Procedures. Polymerization of Hexamethylenediamine and 2,8-Dimethylphenoxathiin-4,6-dicarbonyl Chloride (P1). To a 20 mL scintillation vial equipped with a cap and a magnetic stirring bar were added Na_2CO_3 (113 mg, 1.06 mmol), hexamethylenediamine (49 mg, 98%, 0.42 mmol), and distilled H_2O (2.0 mL). In a separate vessel, **2** (150 mg, 0.425 mmol) was dissolved in CH_2Cl_2 (2.0 mL). This was added to the scintillation vial at room temperature using a pipet with vigorous stirring. A precipitate formed immediately upon addition of the dicarbonyl chloride. The mixture was allowed to stir for an additional 7 h at room temperature and filtered.

The precipitate was washed with H_2O (3×) and MeOH (3×) to give a pale yellow solid which was dried *in vacuo* to yield 141 mg of **P1** (84%). MW (MALDI-TOF): 7000 (DP = 17).

Preparation of P2. To a 50 mL round-bottomed flask were added **17** (172 mg, 91 μmol), DMF, and Et_3N (60 μL, 430 μmol). The mixture was allowed to sit overnight and then evaporated to dryness. The residue was redissolved in DMF (2.0 mL) and diluted with H_2O (5.0 mL) in a 20 mL scintillation vial equipped with a cap and a magnetic stirring bar. Solid Na_2CO_3 (42 mg, 400 μmol) was added. In a separate vessel was dissolved **2** (67 mg, 190 μmol) in CH_2Cl_2 (5.0 mL). This was added to the scintillation vial at room temperature using a pipet with vigorous stirring. A precipitate formed immediately upon addition of the dicarbonyl chloride. The mixture was allowed to stir for an additional 2 h at room temperature and filtered. The precipitate was washed successively with H_2O (3×), CH_2Cl_2 (3×), and MeOH (3×) to give a pale yellow solid which was dried *in vacuo* to yield 120 mg (57%) of **P2**: η_{inh} (dichloroacetic acid) = 0.11 dL/g (concentration = 0.4 g/dL).

Synthesis of Ethylenediamine Octapeptide Polymer P4. To a clean and dry 20 mL scintillation vial equipped with a cap and a magnetic stirrer were added **7b** (773 mg, 1.00 mmol) and anhydrous TFA (3.0 mL) under N_2. Vigorous bubbling was observed immediately. The mixture was allowed to stir for 1.5 h and then evaporated. To the residue was added CH_2Cl_2 (5 mL), and the mixture was again evaporated (repeated 2×). The glassy, light amber residue was taken up in H_2O (5.0 mL), and Na_2CO_3 (530 mg, 5.00 mmol) was carefully added. A solution of **2** (353 mg, 1.00 mmol) in CH_2Cl_2 (5.0 mL) was prepared in a separate vessel and added to the scintillation vial at room temperature via a pipet without stirring initially. After 15 min a thin film formed at the interface, and the mixture was stirred vigorously for 30 min whereupon a heavy precipitate formed. The mixture was directly filtered, and the precipitate was washed successively with MeOH (3×), H_2O (3×), and MeOH (3×). The remaining light yellow solid was dried *in vacuo* to give 393 mg of **P4** (46%): η_{inh} (dichloroacetic acid) = 0.14 dL/g.

Preparation of P3. The procedure for **P4** was followed using **7a** (861 mg, 1.00 mmol) and Na_2CO_3 (1.05 g, 9.92 mmol) in H_2O (5.0 mL) and **2** (353 mg, 1.00 mmol) in CH_2Cl_2 (5.0 mL) to give 470 mg of **P3** (50%) as a pale yellow solid: η_{inh} = 0.19 dL/g.

Synthesis of P5. The procedure for **P4** was followed using **7c** (317 mg, 384 μmol), Na_2CO_3 (321 mg, 3.02 mmol), and **2** (136 mg, 384 μmol) to give 284 mg of **P5** (82%) as a pale yellow solid: η_{inh} = 0.21 dL/g.

2. Solution Polymerization Procedures. Synthesis of P2. To a dried 10 mL round-bottom flask equipped with a magnetic stirrer and a gas-inlet adapter were added **5** (139.4 mg, 135.4 μmol) and anhydrous TFA (1.0 mL) under N_2. Vigorous bubbling was observed immediately. The mixture was allowed to stir for 2.0 h and then evaporated. The residue was further dried *in vacuo* at 70 °C. The TFA salt was taken into a drybox and dissolved in 0.5 mL of 5% LiCl in NMP. To the stirred solution were added diisopropylethylamine (150 mL, 861 μmol) and **2** (47.8 mg, 135.4 μmol). The sides of the flask were washed with 0.5 mL of 5% LiCl in NMP. The polymerization mixture was allowed to stir in the drybox at ambient temperature for 3 days. The mixture was taken out of the drybox and pipetted into 20 mL of distilled H_2O whereupon a white precipitate formed. The mixture was centrifuged at 2500 rpm and the aqueous solution decanted. The residue was washed with H_2O (3×) and MeOH (3×) and dried in a vacuum oven at 80 °C overnight to yield 89.9 mg of a pale yellow solid (**P2**, 60%): T_g 204 °C; $T_{d,onset}$ 313 °C; η_{inh} = 0.16 dL/g. M_n = 19 100; M_w = 39 700; M_p = 42 000 and 14 300 (bimodal); PDI = 2.08.

Synthesis of P4. The above procedure for **P2** was followed using **7b** (302.2 mg, 391.0 μmol), 1.0 mL of 5% LiCl in NMP, diisopropylethylamine (400 μL, 2.30 mmol), **2** (138.1 mg, 391.0 μmol), and an additional 1.0 mL of 5% LiCl in NMP to wash the sides of the flask: yield, 129 mg (39%) of a pale yellow solid; T_g 186 °C; $T_{d,onset}$ 291 °C; η_{inh} = 0.14 dL/g. M_n = 17 400; M_w = 26 900; M_p = 17 200; PDI = 1.54. FABMS: 853.2 (MH^+, cyclic unimer), 1705.5 (MH^+, cyclic dimer).

Synthesis of P5. The procedure for **P4** was followed using **7c** (303.5 mg, 367.0 μmol) and **2** (129.6 mg, 367.0 μmol): yield, 223 mg (67%) of a pale yellow solid; T_g 168 °C; $T_{d,onset}$ 293 °C; η_{inh} = 0.17 dL/g. M_n = 20 200; M_w = 36 200; M_p = 20 800; PDI = 1.79. FABMS: 909.1 (MH^+, cyclic unimer).

Synthesis of P6. The above procedure was followed using a 5 mL round-bottom flask, **7d** (300.6 mg, 329.2 μmol), and **2** (116.3 mg, 329.2 μmol) to give 204 mg of a pale yellow solid (**P6**, 62%): T_g 148 °C; $T_{d,onset}$ 290 °C; η_{inh} = 0.17 dL/g. M_n = 22 300; M_w = 35 600; M_p = 32 500; PDI = 1.60.

Synthesis of P3. The above procedure was followed using **7a** (306.4 mg, 355.9 μmol) and **2** (125.7 mg, 355.9 μmol) to give 187 mg of a pale yellow solid (**P3**, 56%): T_g 156 °C; $T_{d,onset}$ 278 °C; η_{inh} = 0.20 dL/g. M_n = 20 600; M_w = 38 400; M_p = 20 800; PDI = 1.86.

Acknowledgment. We are grateful for financial support from the National Science Foundation under Award No. DMR-9132635, the NSF-supported Cornell University MRL Program under Award No. DMR-9121654, and the Cornell Biotechnology Program National Institutes of Health Trainee Fellowship (M.J.W.). We are also grateful to the DuPont Co. for summer fellowship for M.J.W.

Supporting Information Available: Temperature dependence of amide NH chemical shifts for **13** in both CD_2Cl_2 (500 MHz) and DMSO-d_6 (400 MHz), resolution-enhanced, solid state FTIR (KBr, 2.0 cm^{-1} resolution) of **19**, raw, resolution-enhanced, and second-derivative solid state FTIR spectra of **P5** and **P6**, detailed experimental procedures for the peptides, NMR chemical shift assignments, and FTIR peak listings (14 pages). This material is contained in libraries on microfiche, immediately follows this article in the microfilm version of the journal, can be ordered from the ACS, and can be downloaded from the Internet; see any current masthead page for ordering information and Internet access instructions.

References and Notes

(1) Fraser, R. D. B.; MacRae, T. P. *Conformation of Fibrous Proteins and Related Polypeptides*; Academic Press: New York, 1972; Chapter 13, 14, and 16.
(2) Webster, O. W. *Science* **1991**, *251*, 887.
(3) Krejchi, M. T.; Atkins, E. D. T.; Waddon, A. J.; Fournier, M. J.; Mason, T. L.; Tirrell, D. A. *Science* **1994**, *265*, 1427 and references cited therein.
(4) (a) O'Brien, J. P. *Trends Polym. Sci.* **1993**, *1*, 8. (b) Capello, J.; Crissman, J.; Dorman, M.; Mikolajczak, M.; Textor, G.; Marguet, M.; Ferrari, F. *Biotech. Prog.* **1990**, *6*, 198.
(5) (a) Moser, R.; Klauser, S.; Leist, T.; Langen, H.; Epprecht, T.; Gutte, B. *Angew. Chem., Int. Ed. Engl.* **1985**, *24*, 719. (b) Yang, Y.; Erickson, B. W. *Protein Sci.* **1994**, *3*, 1069 and references cited therein.
(6) (a) Kobayashi, K.; Yonezawa, N.; Katakai, R. *Macromolecules* **1995**, *28*, 8242. (b) Minor, D. L., Jr.; Kim, P. S. *Nature* **1994**, *371*, 264.
(7) (a) Gardner, R. R.; Liang, G.-B.; Gellman, S. H. *J. Am. Chem. Soc.* **1995**, *117*, 3280 and references cited therein. (b) Schneider, J. P.; Kelly, J. W. *J. Am. Chem. Soc.* **1995**, *117*, 2533 and references cited therein. (c) Brandmeier, V.; Sauer, W. H. B.; Feigel, M. *Helv. Chim. Acta* **1994**, *77*, 70. (d) Feigel, M. *Liebigs Ann. Chem.* **1989**, 459. (e) Kemp, D. S.; Stites, N. E. *Tetrahedron Lett.* **1988**, *29*, 5057.
(8) Winningham, M. J.; Sogah, D. Y. *J. Am. Chem. Soc.* **1994**, *116*, 11173.
(9) (a) Nowick, J. S.; Abdi, M.; Bellamo, K. A.; Love, J. A.; Martinez, E. J.; Norohna, G.; Smith, E. M.; Ziller, J. W. *J. Am. Chem. Soc.* **1995**, *117*, 89 and references cited therein. (b) Wagner, G.; Feigel, M. *Tetrahedron* **1993**, *49*, 10831.
(10) Creighton, T. E. *Proteins: Structures and Molecular Properties, 2nd ed.*; W. H. Freeman and Co.: New York, 1993.
(11) Fasman, G. D. In *Prediction of Protein Structure and the Principles of Protein Conformation*; Fasman, G. D., Ed.; Plenum Press: New York, 1989; pp 193−316.
(12) (a) For a review, see: *Silk Polymers: Materials Science and Biotechnology*; Kaplan, D., Adams, W. W., Farmer, B., Viney, C., Eds.; American Chemical Society: Washington, DC, 1994. (b) Wainwright, S. A.; Biggs, W. D.; Currey, J. D.; Gosline,

J. M. *Mechanical Design in Organisms*; Princeton University Press: Princeton, 1976; Chapters 3 and 4.
(13) Urry, D. W. *J. Protein Chem.* **1988**, *7*, 81.
(14) (a) Sogah, D. Y.; Perl-Treves, D.; Voyer, N.; DeGrado, W. F. *Macromol. Symp.* **1994**, *88*, 149. (b) Aoba, T.; Moreno, E. C. In *Surface Active Peptides and Polymers*; Sikes, C. S., Wheeler, A. P., Eds.; American Chemical Society: Washington, DC, 1991; Chapter 7, pp 85−106. (c) Renugopalakrishnan, V.; Pattabiraman, N.; Prabhakaran, M.; Strawich, E. S.; Glimche, M. J. *Biopolymers* **1989**, *28*, 297.
(15) (a) Baer, E.; Moet, A. *High Performance Polymers;* Oxford University Press: New York, 1991. (b) Atkins, E. D. T.; Hill, M.; Hong, S. K.; Keller, A.; Organ, S. *Macromolecules* **1992**, *25*, 917.
(16) (a) Bystrov, V. F. *Prog. Nucl. Magn. Reson. Spectrosc.* **1976**, *10*, 41 and references cited therein. (b) Ramachandran, G. N.; Chandrasekaran, R.; Kopple, K. D. *Biopolymers* **1971**, *10*, 2113.
(17) (a) Tomita, M. *J. Pharm. Soc. Jpn.* **1938**, *58*, 510. (b) Suter, C. M.; McKenzie, J. P.; Maxwell, C. E. *J. Am. Chem. Soc.* **1936**, *58*, 717.
(18) (a) Palmer, B. D.; Boyd, M.; Denny, W. A. *J. Org. Chem.* **1990**, *55*, 438. (b) Gassman, P. G.; Schenk, W. N. *J. Org. Chem.* **1977**, *42*, 918.
(19) (a) Dado, G. P.; Gellman, S. H. *J. Am. Chem. Soc.* **1994**, *116*, 1054 and references cited therein. (b) Ribeiro, A. A.; Goodman, M.; Naider, F. *Int. J. Pept. Protein Res.* **1979**, *14*, 414.
(20) Stevens, E. S.; Sugawara, N.; Bonora, G. M.; Toniolo, G. *J. Am. Chem. Soc.* **1980**, *102*, 7048.
(21) (a) Llinas, M.; Klein, M. P. *J. Am. Chem. Soc.* **1975**, *97*, 4731. (b) Kessler, H. *Angew. Chem., Int. Ed. Engl.* **1982**, *21*, 512.
(22) (a) Zerkout, S.; DuPont, V.; Aubrey, A.; Vidal, J.; Collet, A.; Vicherat, A.; Marraud, M. *Int. J. Pept. Protein Res.* **1994**, *44*, 378. (b) Prasad, S.; Rao, R. B.; Balaram, P. *Biopolymers* **1995**, *35*, 11. (c) Toniolo, C.; Bonora, G. M.; Stavropoulos, G.; Cordopatis, P.; Theodoropoulos, D. *Biopolymers* **1986**, *25*, 281. (d) Aubrey, A.; Chung, M. T.; Marraud, M. *J. Am. Chem. Soc.* **1985**, *107*, 7640. (e) Boussard, G.; Marraud, M. *J. Am. Chem. Soc.* **1985**, *107*, 1825. (f) Sakakibara, S. *Biopolymers* **1995**, *37*, 17.
(23) (a) Yang, H. H. *Aromatic High-Strength Fibers*; John Wiley: Canada, **1989**; pp 111. (b) Go, Y.; Noguchi, J.; Asai, M.; Hayakawa, T. *J. Polym. Sci.* **1956**, *21*, 147. (c) Brack, A.; Spach, G. *Biopolymers* **1972**, *11*, 563. (d) Lotz, B.; Keith, H. D. *J. Mol. Biol.* **1971**, *61*, 201. (e) Mays, J. W. In *Modern Methods of Polymer Characterization;* Barth, H. G., Mays, J. W., Eds.; Wiley-Interscience: New York, **1991**; pp 227−269. (f) Kamide, K.; Saito, M. In *Determination of Molecular Weights*; Cooper, A. R., Ed.; Wiley-Interscience: New York, 1989; pp 145−199.
(24) (a) Montaudo, G.; Garozzo, D.; Montaudo, M. S.; Puglisi, C.; Samperi, F. *Macromolecules* **1995**, *28*, 7983. (b) Mohr, M. D.; Börnsen, K. O.; Widmer, H. M. *Rapid Commun. Mass Spectrom.* **1995**, *19*, 809.
(25) (a) Harris, P. I.; Chapman, D. *Biopolymers* **1995**, *37*, 251. (b) Surewicz, W. K.; Mantsch, H. H. *Biochim. Biophys. Acta* **1988**, *952*, 115.
(26) (a) Bandekar, J.; Krimm, S. *Biopolymers* **1988**, *27*, 885. (b) Bandekar, J.; Krimm, S. *Biopolymers* **1988**, *27*, 909. (c) Susi, H.; Byler, D. M. *Archiv. Biochem. Biophys.* **1987**, *258*, 465. (d) Miyazawa, T.; Blout, E. R. *J. Am. Chem. Soc.* **1961**, *83*, 712. (e) Dong, A.; Huang, P.; Caughey, W. S. *Biochemistry* **1990**, *29*, 3303.
(27) (a) Hempel, A.; Camerman, N.; Camerman, A. *Biopolymers* **1991**, *31*, 187−192. (b) Qian, W.; Bandekar, J.; Krimm, S. *Biopolymers* **1991**, *31*, 193−210.
(28) Odian, G., *Principles of Polymerization*, 3d ed.; Wiley-Interscience: New York, 1991; p 36.

MA960804S